FINAL REPORT

IMAGE DISSECTOR CAMERA SYSTEM STUDY

FEBRUARY 1984

(REVISED MARCH 1984)

Submitted To

NASA
LYNDON B JOHNSON SPACE CENTER
HOUSTON TEXAS 77058

CONTRACT NO. NAS9-16923

AEROSPACE/OPTICAL DIVISION
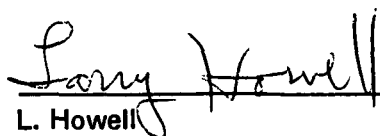3700 E. PONTIAC ST.
P.O. BOX 3700
FORT WAYNE, IN 46801

ITT

FINAL REPORT

IMAGE DISSECTOR
CAMERA SYSTEM
STUDY

FEBRUARY 1984

(REVISED MARCH 1984)

Prepared By:

L. Howell
Project Manager

Submitted To:

NASA
Lyndon B. Johnson Space Center
Houston, Texas 77058

Approved By:

D.J. Juarez
Manager
Electro-Optical Systems Department

Submitted By:

ITT-Aerospace/Optical Division
3700 E. Pontiac Street
P.O. Box 3700
Ft. Wayne, Indiana 46801

ERRATA SHEET

Revision	Date	Pages Affected
A	3-9-84	2-24, 2-25, 2-29, 2-30, 2-31, 3-2, 3-5, R-1

Table of Contents

List of Figures

Section 1

INTRODUCTION

This report was written in response to the tasks outlined in the Statement of Work for The Development of an Infrared Image Dissector (Exhibit A of NASA/JSC Contract No. NAS9-16923).

The report discusses various aspects of a rendezvous and docking system using an image dissector detector as compared to a GaAs detector. Investigation into a gimbled scanning system is also covered and the measured video response curves from the image dissector camera delivered to NASA/JSC on the program are presented.

The design of a rendezvous and docking sensor system must meet the combined requirements of two operating modes. These are (1) search, acquisition, and tracking for rendezvous and (2) tracking for docking. Rendezvous will occur at ranges greater than 100 meters. The maximum range considered here will be 1000 meters. Parameters measured during rendezvous are range, range-rate, angle, and angle-rate of the satellite with respect to the receiver reference. During docking, the range, range-rate, angle, and angle-rate to each reflector on the satellite must be measured. Docking range will be from 3 to 100 meters.

The system to be analyzed consists of a CW laser diode transmitter and an image dissector receiver. The transmitter beam will be amplitude modulated with three sine wave tones for ranging. The beam is coaxially combined with the receiver beam. Mechanical deflection of the transmitter beam, ±10° in both X and Y, can be accomplished before or after it is combined with the receiver beam. The receiver will have a field-of-view (FOV) of 20° and an instantaneous field-of-view (IFOV) of two milliradians (mrad) and will be electronically scanned in the image dissector.

The target spacecraft will be cooperative to the extent that it will maintain an arbitrary but constant attitude (no tumbling) and will have at least three passive reflectors located in a known pattern. Signals from one or more of the reflectors will be used for acquisition and tracking during rendezvous. Signals from each of the reflectors will be used for tracking during docking so that the attitude of the spacecraft can be determined.

The limits and accuracy of the range and angle data required to support rendezvous and docking are given in Tables 1-1 and 1-2, respectively. The target spacecraft will be located, probably by radar, and the range reduced to 1 km. At about this range, acquisition will occur and the rendezvous and docking procedures will be started.

This final report presents the results of analyses in five areas related to a rendezvous and docking investigation. These areas are as follows:

1. A study to determine the advantages to be gained in system performance if a GaAs photocathode is used instead of a multi-alkali photocathode.

2. Determination of laser power requirements versus system performance for the image dissector camera unit delivered on this program.

3. A presentation of the spectral response curves for red sensitive multi-alkali materials and GaAs.

4. Determination of advantages and disadvantages of piezoelectric beam steering and a two-axis-mirror deflection system.

5. Measurement and a record of the frequency response of the image dissector camera.

Table 1-1. Rendezvous Data Requirements

Parameter	Limit	Accuracy (3σ)
Range	0.1 – 1 km	0.01 X Range
Range Rate	± 5 m/s	0.1 m/s
Angle	± .175 rad	10 mrad
Angle Rate	± 5 mrad/s	0.1 mrad/s
Acquisition Time	1s desired	
	5s required	

Table 1-2. Docking Data Requirements

Parameter	Limit	Accuracy (3σ)
Range	3 – 100 m	0.01 X Range
Range Rate	± 1 m/s	0.1 m/s
Angle	± 0.175 rad	10 mrad
Angle Rate	± 5 mrad/s	0.1 mrad/s
Attitude (P,Y)	± 0.5 rad	30 mrad
Attitude (R)	± π rad	30 mrad
Attitude Rate	± 5 rad/s	0.1 mrad/s
Sample Rate	5 samples/s	required
	15 samples/s	desired

Section 2

PHOTOCATHODE STUDY

The photocathode study centered on the following two tasks:

- The determination of the advantages to be gained in the performance of a rendezvous and docking instrument if the GaAs photocathode is developed to replace the existing MA-4 multi-alkali (Sections 2.2 to 2.5).

- The determination of the levels of laser power required for various ranges, tracking rates, and signal-to-noise ratios for the specific image dissector camera that was delivered (Section 2.6).

A secondary task was as follows:

- The presentation of the spectral response curves for the various red sensitive multi-alkali materials and GaAs (Section 2.7).

2.1   SUMMARY OF RESULTS

The use of a GaAs photocathode in place of an MA-4 provides a higher responsivity (sensitivity) R (AW^{-1}). The advantages of changing photocathodes can therefore be gauged from the dependence of the performance parameters on R. The acquisition range depends on $R^{1/8}$ (Section 2.3) and both the range accuracy and angle accuracy on $R^{1/2}$ (Sections 2.4 and 2.5). At the nominal operating wavelength of 830 nm, GaAs has a responsivity that is approximately 5X that of MA-4. As a consequence, its use would increase the acquisition range by $5^{1/8} = 1.22X$ and the tracking accuracy by $5^{1/2} = 2.24X$. This assumes that tracking accuracy is set by random noise and not by other factors.

Nevertheless, the development of a viable production process for building a GaAs photocathode is probably not warranted for two reasons. These are as follows:

- The increase in performance obtained from the substitution of a GaAs photocathode for an MA-4 can also be obtained by increasing either the laser power or the size of the optical elements (receiver or reflector, or both). Moreover, such increases are well within the existing state-of-the-art and do not require the development of any new process or technique.

- The increase in performance obtained from the substitution of a GaAs photocathode for an MA-4 is not needed to meet the present performance requirements of the rendezvous and docking instrument. All of the requirements are

easily met by using an MA-4 photocathode in a conservatively designed system with reasonable laser power levels and with reasonably sized optical elements.

For the present, ITT-A/OD therefore recommends that the best multi-alkali photocathode of the MA-series be used in the rendezvous and docking instrument. However, the development of GaAs is being actively pursued on other current projects in terms of both the production process and the attainment of long life. A switch to GaAs could, therefore, be made at a later time, especially if performance requirements such as acquisition range are more stringent in future applications.

The second reason discussed above is true even if the spread angle of the transmitted beam is increased to allow tracking by the image dissector at all ranges (from acquisition to minimum docking) and the laser power is reduced to a level that can be obtained from a single semiconductor laser. This conclusion is based on the projected ranges of 1,000 m for acquisition and 100 m to 2 m for docking.

If the spread of the transmitted beam is not increased, a point will be reached within the rendezvous and docking operation at which the beam at a retro-reflector is smaller than the reflector aperture. At this distance, it is no longer possible to track the retro-reflector by means of the image dissector. See Section 2.2. It would become necessary to switch to tracking by means of the transmitted beam, i.e., the beamsteerer, at ranges below this point or at all ranges. However, such a switch is not desirable because the transmitter beamsteerer is not as responsive or flexible as that of the image dissector.

An analysis of the requirements for tracking accuracy stated in the RCA study (Table 3-1, p. 23) shows that the instrument design is driven by the specifications on the measurement of angular velocity (angle rate) and radial velocity (range rate) rather than by the specifications on angle and range (Sections 2.5 and 2.6.2). Furthermore, it shows that the limit on tracking rate is set by the accuracy specified on radial velocity rather than angular velocity if the minimum tone wavelength is 20 m (maximum frequency of 15 MHz). Finally, this analysis reveals that the radial velocity accuracy specified for docking requires an inordinately high precision in the phase measurement (~ 1 part in 43,000) if the maximum tone frequency is 15 MHz and measurements (angle and range) on each retro-reflector are needed at the rate of five per second.

To complete the second task (the determination of levels of laser power), it is necessary to design a rendezvous and docking instrument around the specific image dissector that was delivered. This presents some difficulties if all the known requirements are to be met. These are described in Section 2.6. In particular, the F4012 image dissector is too small to cover a 20° x 20° scan field with an f/1, 50 mm receiver lens. In addition, the image dissector aperture is too small to cover an angular diameter of 2 mrad.

Even with these problems, the results of the power level study task confirm those of the photocathode comparison, i.e., that a GaAs photocathode is not needed to meet the performance requirements. For an instrument design as described in Section 2.6, using the delivered image dissector, the acquisition range exceeds 5,000 m at a signal-to-noise ratio of 15 dB and the tracking rates exceed 15 per second during rendezvous and 20 per second during docking, all at the 40 mW power level obtainable from a single semiconductor laser. Moreover, these results are for an instrument in which the transmitted beam angle has been expanded to 30 mrad so that image dissector tracking can be used at all ranges. In the case of docking, ITT-A/OD has increased the allowable radial velocity error to the same level as that specified for rendezvous (0.0033 m/s or 0.075 mph rms) in order to reduce the phase measurement precision to a reasonable level.

2.2   RECEIVER POWER

To evaluate performance during detection and tracking of the retro-reflectors, it is necessary to know the power intercepted by the receiver. The expression for this power depends on the range, which is divided into three regions: far-field, intermediate-field, and near-field. The transition from far- to intermediate-field occurs when either a) the transmitted beam just fills a retro-reflector or b) the return beam from a retro-reflector just fills the receiver aperture. The transition from intermediate to near-field occurs when the remaining aperture (either a, the receiver or b, a retro-reflector) is just filled by the incident beam.

In the far-field, the transmitted beam over-fills the reflector, and tracking is probably done with the detector (image dissector). However, when the range is reduced to the point at which the transmitted beam is smaller than the reflector, the return beam remains at the same angle as long as any portion of the reflector is illuminated. The motions in the reflector, then, can no longer be detected. The beam could move off the retro-reflector and there would be no way to tell which way it went. It is then necessary to either a) track with the transmitter beam by deflecting it in a pattern across the reflector or b) increase the divergence of the transmitted beam to over-fill the reflector at all ranges and continue to track with the detector.

A corner reflector reverses the incident ray in all three dimensions; see Reference 1. There are up-down and right-left, as well as fore-aft, reversals between the incident and reflected rays. As a result, a beam smaller than the reflector and incident near one edge will emerge near the opposite edge. Therefore, a transmitted beam coaxial with the receiver aperture can be displaced as much as one reflector diameter from the receiver axis. However, the tracking eliminates the uncertainty in the position of the reflector produced by this offset in the corner cube.

In addition to the field transitions considered here, there are also transitions at the ranges where the number of reflectors covered by the transmitted beam goes from three to two and from two to one. The latter condition involves two transitions if the reflectors are in an asymmetrical pattern, a condition necessary to remove roll-angle ambiguity. For the reflectors on the circumference of a 1 m diameter circle and for a transmitted beam with a total divergence angle of 2×10^{-3} radian, the first of these transitions is at a range of 500 meters.

2.2.1 Far Field

In the far field, the transmitted beam over-fills a retro-reflector and the reflected beam over-fills the receiving optics. Under the first condition, the power ϕ_f intercepted by the reflector is given by

$$\phi_f = \frac{\phi_t}{r^2} \frac{A_f}{\Omega_t},\tag{1}$$

where

ϕ_t = transmitter (laser) power,

$A_f = \pi D_f^2/4$ = area of the reflector,

$\Omega_t = \pi \theta_t^2/4$ = solid angle of the transmitted beam,

and $\quad$ r = range.

Under the second condition, the power ϕ_r intercepted by the receiver is given by

$$\phi_r = \frac{\phi_f \tau}{r^2} \cdot \frac{A_r}{\Omega_r} = \frac{\phi_t \tau}{r^4} \left(\frac{D_r D_f}{\theta_t \theta_r}\right)^2,\tag{2}$$

where

$A_r = \pi D_r^2/4$ = area of the receiver,

$\Omega_r = \pi \theta_r^2/4$ = solid angle of the reflected beam,

and $\quad$ τ = transmission.

We have included a transmission factor τ in the equation for the received power to account for all the losses between the laser and the detector (image dissector), including any decrease in reflector aperture produced by non-normal incidence of the transmitted beam at the retro-reflector.

The spread angle of the beam reflected from the retro-reflector is equal to the sum of the spread D_f/r in the incident beam and the spread θ_f of the reflector.

$$\theta_r = (D_f/r) + \theta_f. \tag{3}$$

The spread of the incident beam at the reflector is equal to (D_f/r) until the range decreases to the point at which the diameter of the beam is equal to the diameter of the reflector ($\theta_t\, r = D_f$). At ranges less than (D_f/θ_t), the spread of the incident beam is equal to that of the transmitted beam.

The RCA study, see Reference 2, assumes that the divergence from the incident beam is negligible compared with that produced by the reflector, i.e., that

$$(D_f/r) \ll \theta_f.$$

For the nominal values used in the RCA study, $D_r = 5 \times 10^{-2}$ m and $\theta_f = 4 \times 10^{-5}$ radian (diffraction-limited corner cube), this means that $r \gg 1{,}250$ m.

If the far field ends when the return beam decreases to the size of the receiver aperture, we have

$$\theta_r\, r_1 = (\frac{D_f}{r_1} + \theta_f)\, r_1 = D_r, \tag{4}$$

or a range of

$$r_1 = (D_r - D_f)/\theta_f.$$

For $D_r = 0.100$ m, $D_f = 0.050$ m, and $\theta_f = 4 \times 10^{-5}$ radian, this range is

$$r_1 = 1{,}250 \text{ m.}$$

Under these conditions, detection (acquisition) occurs in the far field as long as the required range exceeds 1.25 km.

Under the conditions used in the RCA study, $D_r = D_f = 0.050$ m, so that the transition to the intermediate field is when the size of the transmitted beam matches the reflector.

$$\theta_t\, r = D_f \tag{5}$$

or

$$r = D_f/\theta_t = 0.050/0.002 = 25 \text{ m.}$$

2.2.2   Intermediate Field

When the return beam is equal to or smaller than the receiver aperture, we have

$$\phi_r = \phi_f \ \tau = \frac{\phi_t \ \tau}{r^2} \ (\frac{D_f}{\theta_t})^2 \tag{6}$$

If the transmitted beam becomes equal to or smaller than the retro-reflector aperture, we have

$$\phi_r = \frac{\phi_t \ \tau}{r^2} \ (\frac{D_r}{\theta_r})^2 \tag{7}$$

In either case, the r^{-4} dependence of the received power has been reduced to a r^{-2} dependence. If the intermediate field ends when the size of the transmitted beam matches the reflector, we have

$$\theta_t \ r_2 = D_f \tag{8}$$

or

$$r_2 = D_f / \theta_t = 0.050/0.002 = 25 \ m.$$

This result neglects the size of the transmitted beam at the transmitter/receiver. If the laser beam has a diameter of 2 mm, the match then occurs at r_2 = 24 m.

Under the conditions used in the RCA study, the inter-mediate field ends when the reflected beam matches the receiver, or

$$\theta_r \ r_2 = D_r. \tag{9}$$

Because the transmitted beam at the reflector is smaller than the reflector, the spread of the beam incident on the reflector is now equal to that of the transmitted beam, so that

$$\theta_r = \theta_t + \theta_f = 2.04 \times 10^{-3} \ radian,$$

and

$$r_2 = 24.51 \ m.$$

However, this result again neglects the size of the transmitted beam. If the laser beam has a diameter of 2×10^{-3} m, the reflected beam matches the receiver at a range r_2 that is the solution to

$$2 \times 10^{-3} + 2 \times 10^{-3} \, r + 2.04 \times 10^{-3} \, r = 0.050 \text{ m},$$

or

$$r_2 = 11.88 \text{ m}.$$

Therefore, the intermediate field in the RCA case extends from 11.88 m to 24.51 m.

2.2.3 Near Field

When the transmitted beam is equal to or smaller than the reflector aperture and the reflected beam is equal to or smaller than the receiver aperture, we have

$$\phi_r = \phi_t \, \tau. \tag{10}$$

The received power is then independent of the range r.

Based on the requirements given in the RCA study, see Reference 3, docking begins at 100 m, so that is occurs under both intermediate and near field conditions.

2.3 COMPARISON OF PHOTOCATHODES ON THE BASIS OF ACQUISITION RANGE

It is neither desirable nor necessary to develop a viable production process for building GaAs photocathodes to achieve an acceptable detection (acquisition) range in an operational rendezvous and docking instrument. Increasing the current responsivity (sensitivity) of the photocathode by a factor of 5X (from 0.020 AW^{-1} for an MA-4 to 0.100 AW^{-1} for a GaAs) increases the detection range by a factor of only 1.22X. Moreover, the range of the MA-4 instrument at a signal-to-noise ratio of 15 dB is already in excess of 50 km at a laser transmitter power ϕ_t of one watt.

The limiting noise arises from quantum fluctuations in the background flux. As a result, the signal-to-noise (S/N) power ratio is directly proportional to $\phi_r^2 X R$, where ϕ_r is the received power and R is the photocathode sensitivity. The received power (in the far field), in turn, is directly proportional to r^{-4}, where r is the range (Equation 2). Therefore, for a given S/N, i.e., a given probability of detection, r is directly proportional to $R^{1/8}$. This means that the range depends very weakly on the sensitivity of the photocathode. Moreover, it means that a large difference in photocathode sensitivity can be offset by a modest increase in the sizes of the reflector and receiver, because the range is directly proportional to the square root of the product of their diameters. Therefore, the effect of the 5.0X decrease in R that results from the use of an MA-4 in place of a GaAs photocathode can be eliminated by increasing the diameters of the reflector and receive optics a factor of 1.22X or by 22 percent each.

If a very large acquisition range is not required, then serious consideration should be given to the use of a single diode laser in place of the diode array and beam combiner needed to reach a transmitter power level of one watt. A single AℓGaAs laser diode is capable of reaching an output power level as high as 0.050 W (Reference 4). Even with an MA-4 photocathode, such a reduction in transmitter power still gives us a detection range of 25 km at S/N = 15 dB.

2.3.1   Acquisition

ITT-A/OD assumes that during acquisition the 2 mrad (diameter) transmitter beam is scanned at the rate of 2 radians/sec at a 20 percent overlap, in common with the RCA study (Reference 5). If we are to locate the target within 5 seconds (Reference 6), it must be confined to a field whose diameter ϕ is the solution to

$$\pi \; \phi^2/4 = 2.0 \times 10^{-3} \times 2 \times 5/1.2,$$

or

$$\phi = 0.1456 \text{ radian} = 8.3465°.$$

That is, operation is begun by searching the field around the designated target position. To acquire the target within five seconds under the assumed conditions, its location must be known within a circular field which has a diameter no greater than 8.3465°.

With a transmitter beam diameter of 2 mrad and a scan rate of 2 rads/sec, the dwell time on a target (set of reflectors) in the far field is

$$t = 2 \times 10^{-3}/2 = 1 \times 10^{-3} \text{ sec.}$$

The corresponding noise equivalent bandwidth is

$$\Delta f = 1/2t - 500 \text{ Hz.}$$

This is a factor of 4X smaller than the 2000 Hz used in the RCA study. To obtain the maximum acquisition range, we will assume that the bandwidth is set at 500 Hz.

2.3.2   Other Considerations

In addition to the reduction in noise bandwidth during acquisition (detection), ITT-A/OD has made several other changes to the conditions used in the RCA study to make the design more practical and the analysis more realistic.

  a) The return signal from all three reflectors is detected during acquisition in the far field. The concern over interference phenomena (Reference 5) is without merit. Even if there were interference modulation, it would occur at the carrier frequency and be undetectable in the receiver.

b) The diffuse reflectance (albedo) of the earth background was increased to 40 percent, the average value for the earth (Reference 7). According to Neckel and Labs (Reference 8), the solar spectral irradiance at 830 nm (normal incidence) is 1.068×10^{-1} Wcm^{-2} μm^{-1}. The RCA analysis is therefore based on an albedo of

$$A = 5 \times 10^{-3}/1.068 \times 10^{-1} = 4.68 \times 10^{-2} \cong 4.7 \text{ percent.}$$

Such a low value is seen only in the absence of clouds (Reference 9).

c) The spectral bandwidth of the receiver was increased from 10 nm to 40 nm to accommodate changes in the laser wavelength with temperature, current (modulation), and age. To maintain a more narrow band, we could employ an electronically tunable (optical) spectral filter to track changes in the laser wavelength (References 10 and 11).

d) The receiver diameter, D_r, was set equal to twice the reflector diameter, D_f. This is not a necessary condition, but it is beneficial. Geometrically, i.e., without diffraction at the corner cube, the return beam at the receiver is always twice the size of the reflector when the reflector is over-filled. The received power then depends on r^{-2} rather than r^{-4}. Including the diffraction at the corner cube, this intermediate-field condition is introduced at a much longer range than when $D_r = D_f$ (1,250 m versus 24.5 m for the nominal conditions used in Section 2.2).

2.3.3   Signal/Noise Equation

The number of signal photons in the detected signal from a received (peak) power ϕ_r is given by

$$n_s = \frac{\eta \, \phi_r}{2 \, B \, h \, \upsilon \, \alpha} \tag{11}$$

where

η = quantum efficiency of the photocathode,

B = equivalent noise bandwidth,

h = Planck's constant,

υ = carrier frequency,

α = degradation factor from the modulation and demodulation of the signal = $2\sqrt{2}$.

The variance in the noises from the carrier, background, and dark current in terms of numbers of charge carriers are, respectively,

$$n_c = \frac{\eta \phi_c}{2 B h \nu}$$

$$n_b = \frac{\eta \phi_b}{2 B h \nu}$$

$$n_d = \frac{I_d}{2 B q}$$

and where

ϕ_c = mean carrier power = $\phi_r/2$,

ϕ_b = background power,

I_d = dark current,

and

q = charge on an electron.

The power signal-to-noise ratio is then

$$\frac{S}{N} = \frac{n_s^2}{n_c + n_b + n_d} \tag{12}$$

For the rendezvous and docking instrument, $n_d \ll n_c$, so that we obtain

$$\frac{S}{N} = \frac{(\eta/h\nu) \phi_r^2}{16 B(\frac{1}{2} \phi_r + \phi_b)} \tag{13}$$

The factor $(\eta/h\nu)$ is equal to the current responsivity (sensitivity) R of the photocathode divided by the charge q on an electron. We now have

$$\frac{S}{N} = \frac{R \phi_r^2}{16 B q(\frac{1}{2} \phi_r + \phi_b)} \tag{14}$$

which is the same as the equation on page 96 of the RCA study.

2.3.4   Background Power

The background power detected by the receiver is given by

$$\phi_b = N_\lambda \ \nabla\lambda \ A_r \ \Omega_r' \ \tau_r \tag{15}$$

where

$$N_\lambda = 1.068 \times 10^{-1} \ a/\pi \ \mathrm{Wcm}^{-2} \ \mathrm{ster}^{-1} \ \mu\mathrm{m}^{-1},$$

$$\nabla\lambda = 40 \times 10^{-3} \ \mu\mathrm{m},$$

$$a = \mathrm{albedo} = 0.40,$$

$$A_r = \pi D_r^2/4, \ D_r = \text{receiver optics diameter} = 10 \ \mathrm{cm},$$

$$\Omega_r' = \pi \ \theta_r^2/4, \ \theta_r = \text{receiver field-of-view diameter} = 2 \times 10^{-3} \ \mathrm{radian},$$

and

$$\tau_r = \text{receiver transmittance} = 0.50.$$

We therefore have

$$\phi_b = 6.7104 \times 10^{-8} \ \mathrm{W}.$$

2.3.5 Detection Range

In common with the RCA study, ITT-A/OD will define detection as the point where the power signal-to-noise ratio $S/N = 31.62$ or 15 dB. For

$$B = 500 \ \mathrm{Hz},$$

$$q = 1.602 \times 10^{-19} \ \mathrm{coulomb},$$

$$\phi_b = 6.7104 \times 10^{-8} \ \mathrm{W},$$

$$R = 0.100 \ \mathrm{AW}^{-1} \ (\mathrm{GaAs}), \ 0.020 \ \mathrm{AW}^{-1} \ (\mathrm{MA\text{-}4}),$$

we obtain

$$31.62 = \frac{(0.100, \ 0.020) \ \phi_r^2}{1.2816 \times 10^{-15}(0.5 \ \phi_r + 6.7104 \times 10^{-8})}$$

Solving for ϕ_r, we obtain

$$\phi_r = 1.6501 \times 10^{-10} \ \mathrm{W(GaAs)}, \ 3.6924 \times 10^{-10} \ \mathrm{W(MA\text{-}4)}.$$

In both cases, we see that $0.5 \ \phi_r \ll \phi_b$, so that the sensitivity is limited by the quantum fluctuations in the background.

We are now in a position to determine the ranges that correspond to the above received powers. In the far field, where

acquisition occurs, the power received from all three reflectors is given by (Equation 2)

$$\phi_r = 3\frac{\theta_t \, \tau}{r^4} \left(\frac{D_r \, D_f}{\theta_t \, \theta_r}\right)^2,$$

where

ϕ_t = transmitter (laser) power = 1 W,

τ = transmittance from laser to detector = 0.25,

D_r = 0.100 m,

D_f = reflector diameter = $\frac{1}{2} D_r$ = 0.050 m,

r = range,

θ_t = angular diameter of the transmitter beam = 2×10^{-3} radian,

θ_r = angular diameter of the reflected beam = divergence angle of the corner cube under far-field conditions = 4×10^{-5} radian.

We therefore have

$$\theta_r = 2.9297 \times 10^9 \, r^{-4} \text{ W, r in meters}$$

and

$$r = 64.91 \text{ km (GaAs)}, \ 53.07 \text{ km (MA-4)}.$$

Substitution of the above aquation for ϕ_r into the S/N equation shows us that under background-limited conditions $(0.5 \ \phi_r \ll \phi_b)$ the detection range in proportional to

$$r \ \alpha \ \phi_t^{1/4} \ \tau^{1/4} \ R^{1/8} \ (D_f \, D_r / \theta_t \, \theta_r)^{1/2}.$$

Changing from an MA-4 to a GaAs photocathode, therefore, increases the range by $(5)^{1/8}$ = 1.223X, or from 53.1 km to 64.9 km in the above example. Such an increase can also be obtained by increasing both the reflector (D_f) and receiver (D_r) diameters by 22.3 percent. We also see that, if the laser power is reduced from 1 W to 0.050 W, a level that can be obtained from a single diode, the range is reduced by a factor of $(0.050)^{1/4}$ = 0.4729X, or 30.7 km for a GaAs and 25.1 km for an MA-4 receiver.

2.4 COMPARISON OF PHOTOCATHODE ON THE BASIS OF RANGE ACCURACY

In common with a comparison made on the basis of acquisition range (Section 2.3), a comparison of photocathodes on the basis of the accuracy of range measurements shows that there is no need to develop GaAs photocathodes for use in an operational rendezvous and docking instrument. The accuracy of a range measurement depends on the square root of the photocathode responsivity (sensitivity), i.e., $R^{1/2}$, rather than the $R^{1/8}$ dependence of the acquisition range. As a result, substitution of a GaAs photocathode for an MA-4 would increase range accuracy by approximately $5^{1/2} = 2.24$. Such an increase can be offset by increasing the transmitted laser power by $5^{1/4} = 1.50$ (under background-noise-limited conditions) or the diameters of both the retro-reflector and receiver optics by $5^{1/8} = 1.22$. However, there is no need for such increases at the anticipated maximum rendezvous (tracking) range of 1000 m or the maximum docking range of 100 m. As shown by the sample calculations given in Section 2.4.4, the range accuracy requirements can be met using the delivered MA-4 photocathode $(R \approx 0.016 \text{ A W}^{-1})$. This is true even when the transmitted beam is expanded (to 30×10^{-3} radian) to allow detector tracking at all ranges and the laser power is reduced to the level $(40 \times 10^{-3} \text{ W})$ available from a single semiconductor laser.

ITT-A/OD assumes that range is determined from a measurement of the phase shift in one or more amplitude modulated tones, as described in Section 4.8 of the RCA study. Phase may be measured by either coherent demodulation (Section 2.4.1) or zero-crossing detection (Section 2.4.2). In either case, the rms error in the range measurement is given by

$$\delta r = \frac{\lambda}{4\pi (S/N)^{1/2}},$$

where λ is the tone wavelength and (S/N) is the power signal-to-noise ratio. Using Equation 14 for (S/N), we see that δr depends on the current responsivity (sensitivity) R of the image dissector photocathode according to

$$\delta r \propto R^{1/2}.$$

The equation for δr also shows us that the accuracy of the range measurement can be increased by the use of multiple tones (Section 2.4.4). The reduction in $(S/N)^{1/2}$ that results from the use of more than one tone, i.e., the division of the laser power, is more than offset by the accompanying reduction in the (lowest) tone wavelength λ.

2.4.1 Phase Measurement by Coherent Demodulation

In this approach to phase measurement, a reference from the transmitted signal is used to coherently (synchronously) demodulate the received signal. The reference or transmitted signal may be expressed by

$$S_t = A_t \cos x, \tag{16}$$

and the received signal by

$$S_r = A_r \sin(x + \phi), \tag{17}$$

where ϕ is the phase shift to be measured. Synchronous demodulation is equivalent to multiplication, so that the output can be expressed by

$$0 = S_t \, S_r = A_t \, A_r \sin(x + \phi) \cos x$$

Using the relationship

$$\sin u \cdot \sin v = \tfrac{1}{2}(\sin (u - v) + \sin (u + v),$$

this becomes

$$0 = \tfrac{1}{2} A_t \, A_r \, (\sin \phi + \sin (2x + \phi).$$

A low-pass filter is then used to recover the dc signal, which is

$$0_{dc} = \tfrac{1}{2} A_t \, A_r \sin \phi. \tag{18}$$

The phase to be determined is then the solution to

$$\sin \phi = \frac{0_{dc}}{\tfrac{1}{2} A_t \, A_r}.$$

For small ϕ, this becomes

$$\phi = \frac{0_{dc}}{\tfrac{1}{2} A_t \, A_r} \tag{19}$$

The phase is related to the range by

$$\phi = 2\pi \cdot \frac{2r}{\lambda} = \frac{4\pi r}{\lambda}, \tag{20}$$

where λ is the wavelength of the tone. The error δr in a range measurement is then related to the uncertainty $\delta 0_{dc}$ in the demodulated and filtered output by

$$\frac{4 \pi \, \delta r}{\lambda} = \frac{\delta 0_{dc}}{\tfrac{1}{2} A_t \, A_r} \tag{21}$$

Now we can equate the uncertainty $\delta 0_{dc}$ to the rms output noise (voltage or current) N, which is given by

IDCA-16

$$N = \tfrac{1}{2} A_t \sqrt{2} N_O \qquad (22)$$

where N_O is the noise in a band-pass B. The factor A_t is from the demodulation (reference) waveform, $\tfrac{1}{2}$ from the sin u · sin v relationship, and $\sqrt{2}$ from the fact that the noise in a band 2B, i.e., $\pm$ B about the tone frequency, contributes to the final output noise. We now have

$$\frac{4 \pi \delta r}{\lambda} = \frac{\sqrt{2} N_O}{A_r}. \qquad (23)$$

However, the ratio in the right side is just the reciprocal of the square root of the signal-to-noise (power) ratio, so that

$$\frac{4 \pi \delta r}{\lambda} = \frac{1}{(S/N)^{1/2}} \qquad (24)$$

which is the same as the expression given in the RCA study (page 44). The amplitude A_r of the received signal is related to the (peak) received laser power ϕ_r by $A_r = \tfrac{1}{2} R \phi_r$, where R is the responsivity (sensitivity) of the image dissector photocathode; the noise power in a frequency band B is given by

$$N_O^2 = 2 Bq (\tfrac{1}{2} \phi_r + \phi_b) R,$$

where q is the charge on an electron and ϕ_b is the background (solar illuminated earth) power. That is, (S/N) is given by Equation 14 in Section 2.3.3.

2.4.2   Phase Measurement by Zero-Crossing Detection

The range can also be determined by measuring the time difference (delay or phase shift) between the reference (transmitted) and received signals as a positive-slope zero-crossing (or other fixed point) in the sinusoidal waveform. If the received signal is expressed as a sinewave,

$$S = A_r \sin (2 \pi f t), \qquad (25)$$

an uncertainty in time δt is related to an uncertainty in amplitude δS by

$$\delta S = 2 \pi f A_r \cos(2 \pi f t) \delta t,$$

or

$$\delta t = \frac{\delta S}{2 \pi f A_r \cdot \cos 2 \pi f t}. \qquad (26)$$

IDCA-17

For a zero-crossing of the sinewave, $2\pi f t = 2\pi n$ and $\cos 2\pi f t = 1$, so that

$$\delta t = \frac{\delta S}{2\pi f A_r}. \tag{27}$$

The wavelength λ of the tone signal is related to its frequency f by $f = c/\lambda$, where c is the velocity of light; and the error in range is related to the uncertainty in time by $c\, \delta t = 2\, \delta r$. We therefore have

$$\frac{2\, \delta r}{c} = \frac{\lambda\, \delta S}{2\pi c A_r},$$

or

$$\delta r = \frac{\lambda\, \delta S}{4\pi A_r} = \frac{\lambda}{4\pi\, (S/N)^{1/2}},$$

where we have identified the uncertainty δS in the signal level with the rms noise (voltage or current) in the frequency band $\pm$ B about the tone frequency.

When phase is determined by coherent demodulation, the measurement bandwidth B is just the bandwidth of the output, low-pass filter. When the range is determined from a zero-crossing measurement of a signal with a modulation (tone) frequency f, the phase is measured once each wavelength or at a time interval $\Delta t_1 = 1/f$. However, there is a total time Δt in which to determine the range, so that it is based on a total of n measurements, where $n = \Delta t \cdot f$. The effective noise bandwidth is then

$$\frac{1}{2n\, \Delta t_1} = \frac{f}{2\, \Delta t \cdot f} = \frac{1}{2\, \Delta t},$$

or the same as for coherent demodulation.

2.4.3   Multiple-Tone Operation

From the above equation, we see that the range error δr can be reduced by using a shorter wavelength (higher frequency) tone signal. However to make an unambiguous measurement, the total distance 2r traveled by the tone signal cannot exceed the wavelength of the tone, i.e.,

$$2r < \lambda. \tag{29}$$

In terms of frequency, this becomes

$$f < c/2r,$$

where c is the velocity of light. This relationship is given as a maximum tone frequency in the RCA study, (page 38).

In order to overcome this limitation, multiple tones are used. For simultaneous measurements, this divides the laser power among the tones and therefore reduces the signal-to-noise ratio. However, this is more than offset by a reduction in λ, so that a reduction in δr is realized.

The wavelength (or frequency) ratio between tones is set by the accuracy with which the phase can be measured. Using equations 20 and 24, the rms error $\delta\phi$ in the phase measurement is given by

$$\delta\phi = \frac{2\pi}{\lambda} \delta r = \frac{1}{(S/N)^{1/2}} \tag{30}$$

In terms of the first tone wavelength λ_1, this is

$$\frac{\delta\lambda_1}{\lambda_1} = \frac{\delta\phi}{2\pi} = \frac{1}{2\pi (S/N)^{1/2}}. \tag{31}$$

The next lower wavelength λ_2 can then be set by a criterion such as

$$\lambda_2 > 3 \; \delta\lambda_1,$$

or

$$\lambda_2 > \frac{3\lambda_1}{2\pi (S/N)^{1/2}}. \tag{32}$$

Suppose, for example, that we used two tone frequencies combined with the criterion $\lambda_2 = 4\lambda_1/2\pi (S/N)^{1/2}$. The error in range measurement is now given by

$$\delta r_2 = \frac{\lambda_2}{4\pi (S/N)_2^{1/2}} = \frac{4\lambda_1}{8 \pi^2 (S/N)_2}.$$

We then have

$$\frac{\delta r_2}{\delta r_1} = \frac{2(S/N)_1^{1/2}}{\pi (S/N)_2}.$$

If the laser power is equally divided between the two tones, $(S/N)_2 = \frac{(S/N)_1}{4}$ (see Equation 14). We therefore have

$$\frac{\delta r_2}{\delta r_1} = \frac{4(S/N)_1^{1/2}}{\pi (S/N)_1} = \frac{4}{\pi (S/N)_1^{1/2}}.$$

2-17

IDCA-19

The accuracy is then improved, i.e., $\delta r_2/\delta r_1 < 1$, as long as $(S/N)_1^{1/2} > 4/\pi = 1.27$ (1.05 dB).

2.4.4   Sample Calculations

We will assume that the spread angle θ_t of the transmitted beam has been increased to 3×10^{-2} radian to allow detector tracking down to a minimum range of $D_f/\theta_t = 0.050/3 \times 10^{-2} = 1.67$ m. We can then track by means of the detector at all the ranges to be covered, from the maximum acquisition range (1×10^3 m) to the minimum docking range (2 m). In addition, we will assume that the laser power ϕ_t has been reduced to 4×10^{-2} W, a level obtainable from a single semiconductor laser. If the rest of the system has the same optical design as that used to calculate detection range in Section 2.3.5, we also have

$$D_r = 0.100 \text{ m},$$

$$D_f = 0.050 \text{ m}$$

$$\theta_r = \frac{D_f}{r} + \theta_f = \frac{0.050}{r} + 4 \times 10^{-5},$$

and

$$\tau = 0.25.$$

From the calculations given in Section 2.3.4, the background power detected by the receiver is $\phi_b = 6.7104 \times 10^{-8}$ W. Finally, we will assume that the laser power ϕ_t is equally divided between two tone frequencies and that the photocathode has a responsivity $R = 0.016$ A W^{-1}, the same as the delivered MA-4 image dissector.

For the above design, the system is operating in the intermediate field at all the distances to be covered (See Section 2.2.2). At a maximum tracking (rendezvous) range r of 1×10^3 m, the received signal from three retro-reflectors and one tone frequency is then, from equation 2,

$$\phi_r = 3 \frac{2 \times 10^{-2} \times 0.25}{(1 \times 10^3)^2} \left(\frac{0.05}{3 \times 10^{-2}}\right)^2,$$

or

$$\phi_r = 4.167 \times 10^{-8} \text{ W}.$$

We can now calculate the signal-to-noise ratio from Equation 14 by setting the equivalent noise bandwidth B. If the measurement rate is set at five per second (Reference 6), a total time interval $\Delta t = 0.20$ seconds is available for the measurement of azimuth angle, elevation angle, and range and the tracking of the target. If the time is equally divided among these four, the bandwidth becomes

$$B = \frac{4}{2 \, \Delta t} = 10 \text{ Hz.}$$

For $R = 0.016 \text{ A W}^{-1}$, we now have

$$\frac{S}{N} = \frac{0.016 \, (4.167 \times 10^{-8})^2}{16 \times 10 \times 1.602 \times 10^{19} (4.167 \times 10^{-8} + 6.7104 \times 10^{-8})}$$

or

$$\frac{S}{N} = 9.963 \times 10^6 = 70.0 \text{ dB}$$

Note that, as shown in the calculation, the variance (noise power) from both tone signals appears in the output.

To meet the requirement of Equation 29, the longer tone wavelength must satisfy $\lambda_1 > 2 \times 10^3$ m. If we select $\lambda_1 = 2.2 \times 10^3$ m and $\lambda_2 = 0.1 \, \lambda_1 = 2.2 \times 10^2$ m, the rms error in the range measurement becomes, from Equation 28,

$$\delta r = \frac{2.2 \times 10^2}{4\pi (9.963 \times 10^6)^{1/2}} = 5.55 \times 10^{-3} \text{ m,}$$

so that $3\delta r/4 = 1.66 \times 10^{-5}$. This is less than both of the requirements given in the RCA study (0.01 in Table 2-3, page 10 and 1.5×10^{-4} in Table 3-1, page 23). Finally, the uncertainty in the measurement of the longer wavelength is, from Equation 31,

$$\delta\lambda = \frac{2.2 \times 10^3}{2\pi (9.963 \times 10^6)^{1/2}} = 1.11 \times 10^{-1} \text{ m,}$$

or 0.050 percent of the shorter wavelength (220 m).

During docking, the bandwidth B is increased by a) the need to track at least three retro-reflectors and b) the step and settle time of the beam steerer moving between the reflectors. If the step and settle time between two reflectors is equal to the total time on a reflector, the bandwidth is increased to $2 \times 3 \times 10 = 60$ Hz. At the maximum docking range of $r = 100$ m , the received signal for each tone is now

$$\phi_r = \frac{2 \times 10^{-2} \times 0.25}{(1 \times 10^2)^2} \left(\frac{0.05}{3 \times 10^{-2}}\right)^2$$

or

$$\phi_r = 1.389 \times 10^{-6} \text{ W.}$$

IDCA-21

The corresponding signal-to-noise ratio is

$$\frac{S}{N} = \frac{0.016 \ (1.389 \times 10^{-6})^2}{16 \times 60 \times 1.602 \times 10^{-19}(1.389 \times 10^{-6} + 6.7104 \times 10^{-8})},$$

or

$$\frac{S}{N} = 1.378 \times 10^8 = 81.4 \ dB.$$

The rms error in the range measurement is then

$$\delta r = \frac{2.2 \times 10^2}{4\pi \ (1.378 \times 10^8)^{1/2}} = 1.49 \times 10^{-3} m = 1.49 \ mm,$$

so that $3\delta r = 4.47$ mm and $3\delta r/r = 4.47 \times 10^{-5}$. These errors are well below both of the docking requirements listed in the RCA study (15 mm in Table 3-1, page 23, and 0.01 in Table 204, page 11).

2.5   COMPARISON OF PHOTOCATHODES ON THE BASIS OF ANGLE ACCURACY

The results of a comparison of GaAs and MA-4 photocathodes on the basis of angle accuracy are the same as a comparison on the basis of range accuracy; see Section 2.4. The accuracy of an angle measurement depends on the square root of the photocathode responsivity ($R^{1/2}$), and the increased accuracy obtained with GaAs photocathode can be offset with the increases in laser power or optics diameter, or both. Once again, however, there is no need for such an offset. The angle accuracy requirements are easily met by using an MA-4 photocathode, even when the angle of the transmitted beam is increased (to 30 mr) for detector tracking at all positions and the laser power is reduced to the level (40 mW) of a single semiconductor laser. This conclusion is based on the projected maximum tracking range of 1000 m and the projected docking range of 100 m to 2 m.

We will assume that the angular position (bearing) of a target is determined by scanning the received signal spot with the image dissector aperture in two orthogonal directions. As shown in Figure 2.5-1, the angle in a given direction is determined from the measurement of the two half-amplitude points, according to

$$\theta_m = \frac{1}{2}(\theta_2 - \theta_1) \qquad\qquad (33)$$

The variance in this measurement is given by

$$(\delta \ \theta_m)^2 = \frac{1}{4}(\delta \ \theta_2)^2 + \frac{1}{4}(\delta \ \theta_1)^2.$$

For $\delta \ \theta_2 = \delta \ \theta_1 = \delta \ \theta$, we then have an rms error of

$$\delta \ \theta_m = \frac{\delta\theta}{\sqrt{2}}$$

From Figure 2.5-1, we also have

$$\frac{\delta\theta}{\delta S} = \frac{\theta}{S}$$

where θ is the ramp angle and S is the signal. This gives us

$$\delta\,\theta_m = \frac{\theta}{\sqrt{2}(S/N)^{1/2}}, \tag{34}$$

where we have identified the uncertainty δS in the signal level with the rms noise (voltage or current).

At the maximum rendezvous range of 1000 m, the ramp angle θ is equal to the angular diameter θ_r of the reflected beam. For the system parameters used in our sample calculations (Section 2.4.4), $\theta_r = 9 \times 10^{-5}$ and $(S/N) = 9.963 \times 10^6$, so that

$$\delta\,\theta = 2.02 \times 10^{-5}\ \text{mr},$$

and

$$3\delta\,\theta = 6.05 \times 10^{-5}\ \text{mr}.$$

This is much less than the required accuracies listed in the RCA study (10 mrad and 1.2 mrad, Tables 2-3 and 3-1). However, the above uncertainty represents only the random error of the detection noise. At such a low noise level, the actual accuracy may be set by other sources, such as errors in the angular calibration of the receiver (offset or bias errors) and changes in the operating characteristics of the image dissector over time and temperature.
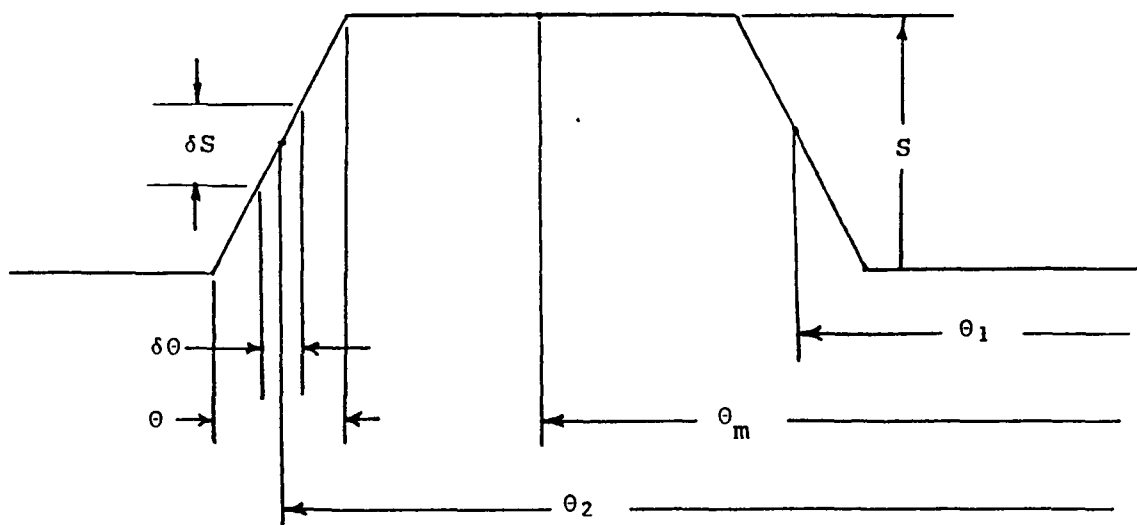

Figure 2.5-1. Measurement of Angular Position

An obvious source of additional error is the movement of the target during the measurement period. If an angular measurement takes 0.050 seconds and the target has an angular velocity of 1 mrad/s, the target will move by 0.050 mrad during the measurement. However, this error can be corrected by use of the measured angular velocity. In fact, the angular and radial velocities must be used during docking to correct the measurements from the three targets to a common time reference.

At the maximum docking range of 100 m, we have (Section 2.4.4) $\theta_r = 5.4 \times 10^{-4}$ and $(S/N) = 1.378 \times 10^8$, so that

$$\delta\theta = 3.25 \times 10^{-5} \text{ mr,}$$

and

$$3\delta\theta = 9.76 \times 10^{-5} \text{ mr.}$$

This is also well below the 1.2 mrad requirement given in the RCA report (Table 3-1).

As the range is decreased below 100 m, we may reach a point at which the angle θ_r of the reflected beam becomes equal to angle θ_d of the image dissector aperture. The value of θ_d must then be substituted for θ_r in the equation for the rms error in the measurement of the angle. For $\theta_d = 2 \times 10^{-3}$, this cross-over occurs at a range r_c that is the solution to

$$\theta_r = \theta_f + \frac{D_f}{r_c} = \theta_d, \tag{35}$$

or

$$r_c = \frac{D_f}{\theta_d - \theta_f} + \frac{0.050}{2 \times 10^{-3} - 4 \times 10^{-5}} = 25.51 \text{ m.}$$

Finally, we would like to point out that the angle and angle rate accuracy requirements given in the RCA study appear to be inconsistent, at least for a measurement rate of five per second. The angular velocity is calculated from two angle measurements according to

$$\omega = \frac{\Delta\theta}{\Delta t} = \frac{\theta_{m1} - \theta_{m2}}{\Delta t}, \tag{36}$$

where Δt is the time interval between the measurements. The mean square error in a velocity measurement is then

$$(\delta\omega)^2 = \frac{1}{(\Delta t)^2} (2 \langle\delta\theta\rangle^2 + \omega^2 \langle\delta t\rangle^2),$$

IDCA-24

where δt is the rms error in the time interval Δt. By the use of a high frequency reference clock, we can make $\omega\,(\delta t) \ll \delta\,\theta$, so that

$$\delta\,\omega = \frac{\sqrt{2}\ \delta\,\theta}{\Delta t},$$

or

$$\delta\,\theta = \frac{\delta\,\omega\,\Delta t}{\sqrt{2}}. \tag{37}$$

Using the performance requirements listed in Table 3-1 of the RCA study, $3\delta\,\omega = 0.1$ mrad/second. If measurements are made at the rate of five per second, $\Delta t = 0.20$ seconds, and the required angle accuracy is

$$3\delta\,\theta = \frac{0.1 \times 0.2}{\sqrt{2}} = 1.41 \times 10^{-2}\ \text{mrad}.$$

This is a factor of approximately 85 smaller than the listed angle accuracy of 1.2 mrad. A similar inconsistency is apparent between the listed range and the range rate accuracies.

2.6   LASER POWER REQUIREMENTS

In order to determine the levels of laser power required for various acquisition ranges, tracking rates, and signal-to-noise ratios for the specific image dissector unit that was delivered, we have to assume values for the system parameters outside of the dissector itself. To begin with, we will assume that the receiver aperture has a diameter D_r of 0.050 m. In order to cover as large a scan field as possible, the focal length and, therefore, the f-number must be as small as possible. A practical lower limit is f/1, setting the focal length at 50 mm. Because the F4012 image dissector has a quality circle diameter of 0.56 inches, the receiver then covers a total scan field which has a diameter of

$$\psi = 2\ \arctan \frac{0.56 \times 25.4}{2 \times 50} = 16.2°$$

This corresponds to a square field, 11.4° on a side. In order to operate down to a minimum docking range of 2 m, the retro-reflectors must then be within a circle which has a diameter of 0.57 m.

In addition to an MA-4 photocathode with a responsivity R = 0.016 AW^{-1}, at a wavelength of 830 nm, the delivered image dissector also has an aperture with a 0.98×10^{-3} inch diameter. For the above receiver optics, this provides a receiver (detector) angle of

$$\theta_d = \frac{0.98 \times 10^{-3}}{0.56} \times \psi \times \frac{\pi}{180°} = 0.49 \times 10^{-3} \text{ radian.}$$

As a result, the return signal completely fills the dissector aperture when the range is reduced to a level r_c that satisfies

$$\theta_r = \theta_f + \frac{D_f}{r_c} = \theta_d = 0.49 \times 10^{-3} \text{ radian}$$

where θ_f is the spread angle of a retro-reflector and D_f is its diameter. For $\theta_f = 4 \times 10^{-5}$ (diffraction-limited corner cube) and $D_f = 0.050$ m, we obtain

$$r_c = 110 \text{ m.}$$

This means that within the entire docking range, $2 \text{ m} \leq r \leq 100 \text{ m}$, the detector aperture is smaller than the spot size of the return signal, and the received signal power is reduced by the factor

$$(\theta_d/\theta_r)^2.$$

2.6.1   Detector Range

For the instrument design described above and a spectral bandwidth of 40 nm, the background power is (Section 2.3.4)

$$\phi_b = 0.1068 \times \frac{0.4}{\pi} \times 4 \times 10^{-2} \times \frac{\pi(5.0)^2}{4} \times \frac{\pi(0.49 \times 10^{-3})^2}{4} \times 0.5$$

$$= 1.007 \times 10^{-9} \text{ W,}$$

where we have assumed that the background has an albedo of 0.40 (the average for the earth) and is illuminated by normally incident sunlight. For an acquisition scan rate of two radians/second and a receiver beam diameter of 0.49×10^{-3} radian, the dwell time on a target is $t = 2.45 \times 10^{-4}$ s, which results in an equivalent noise bandwidth $B = \frac{1}{2}t$ or 2.04×10^3 Hz, see Section 2.3.1. As in Section 2.3.5, we will define target detection as occurring when the power signal-to-noise ratio is 31.62 or 15 dB. From Equation 14 in Section 2.3.3, we therefore have

$$\frac{S}{N} = 31.62 = \frac{0.016 \, \phi_r^2}{16 \times 2.04 \times 10^3 \times 1.602 \times 10^{-19}(0.5 \, \phi_r + 1.007 \times 10^{-9})}$$

Solving for the required received power, we obtain

$$\phi_r = 1.046 \times 10^{-10} \text{ W.}$$

We now have to relate ϕ_r to the laser power ϕ_t and the range r. In order to do this, we must select a spread angle θ_t for the transmitted beam. We will use $\theta_t = 3 \times 10^{-2}$ to allow detector tracking down to the minimum range of 2 m. In addition, we will assume that the signals from all three reflectors are detected at acquisition. At a minimum acquisition range of 1000 m with the 0.49 mrad receiver angle, this requires that the reflector lie within a circle which has a diameter of 0.49 m. For an end-to-end transmission $\tau = 0.25$, this gives us (Section 2.3.5).

$$\phi_r = 1.046 \times 10^{-10} = \frac{3 \times 0.25 \; \phi_t}{r^4} \left(\frac{0.050 \times 0.050}{3 \times 10^{-2} \; (\frac{0.050}{r} + 4 \times 10^{-5})} \right)^2$$

The laser power that results and is required for various detection ranges are plotted in Figure 2.6.1-1 and listed in the following tabulation:

Detection Range r (m)	Laser Power ϕ_t (W)
12.5×10^3	9.49×10^{-1}
12×10^3	8.13×10^{-1}
10×10^3	4.07×10^{-1}
8×10^3	1.76×10^{-1}
6×10^3	6.08×10^{-2}
5×10^3	3.14×10^{-2}
4×10^3	1.42×10^{-2}
3×10^3	5.22×10^{-3}
2×10^3	1.36×10^{-3}
1.5×10^3	5.47×10^{-4}
1×10^3	1.63×10^{-4}

$N_\lambda = 1.068 \times 10^{-1}$ a/π Wcm^{-2}ster^{-1} μm^{-1} $D_r = 0.050$ m, $D_f = 0.050$ m

$a = 0.40$, $\Delta\lambda = 40 \times 10^{-3}$ μm $R = 0.016$ AW^{-1}, $\beta = 2.04 \times 10^3$ Hz, $\tau = 0.25$

$\theta_d = 0.49 \times 10^{-3}$, $\tau_r = 0.50$ $\theta_t = 3 \times 10^{-2}$, $\theta_f = 4 \times 10^{-5}$
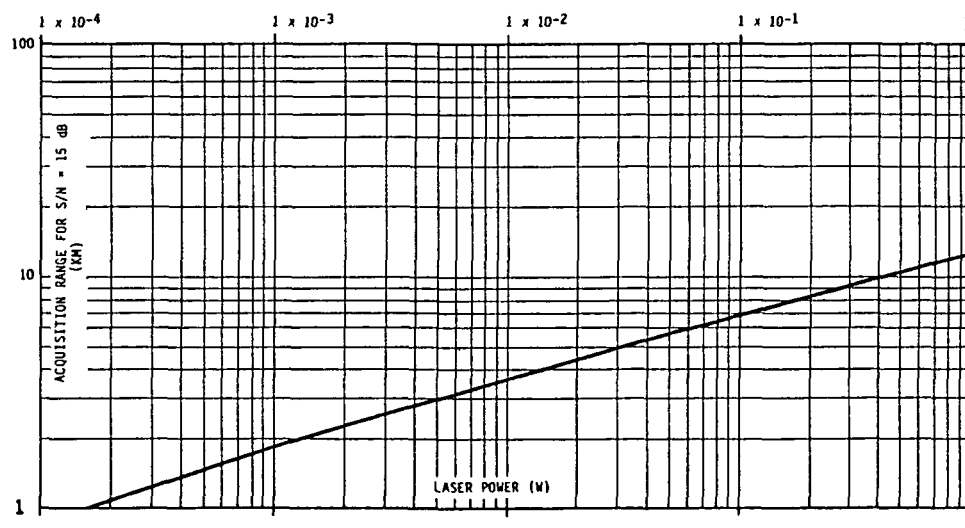

Figure 2.6.1-1. Laser Power Versus Acquisition Range

2.6.2 Tracking Rates

The tracking rate may be taken as $1/\Delta t$, where Δt is the time interval between two sets of measurements on a target (angular position and range). In addition, tracking requires that we measure the angles and range to a specified accuracy. If the tracking rate has a minimum value of five per second, then the accuracy requirements for both angle and range are set by the specified rate accuracy rather than the amplitude accuracy. This conclusion is based on the performance requirements listed in Table 3-1, page 23, of the RCA study. We have already shown that this is true for the angle measurements (Section 2.5). A similar result holds for range.

Using a derivation similar to that given in Section 2.5 for angle measurements, we find that the rms range error required for a range data (radial velocity) rms error δV_r is given by

$$\delta r = \frac{\delta V_r \, \Delta t}{\sqrt{2}}. \qquad (38)$$

This result assumes that the contribution from the error in measuring the time interval Δt is negligible. For $v_r > 1$ m/s (rendezvous), $3\delta v_r = 0.1$ m/s, so that for $\Delta t = 0.20$ s, $\delta r = 4.7 \times 10^{-3} = 4.7$ mm and $3\delta r = 14.1$ mm. This is less than the 1.5×10^{-4} r listed as the 3σ range accuracy requirement during rendezvous. However, it is very nearly the same as the range accuracy requirement ($3\delta r = 15$ mm) at the minimum rendezvous range of 100 m, which is the same as the range accuracy specified for docking. During docking ($v_r \leq 1$ m/s), on the other hand, the value listed for $3\delta v_r$ is 0.01 m/s, so that the corresponding δr level is reduced to 0.47 mm. This means that the wavelength and, therefore, the phase would have to be measured to an accuracy of

$$\frac{\delta\phi}{2\pi} = \frac{\delta\lambda}{\lambda} = \frac{4.7 \times 10^{-4}}{20} = \frac{1}{42,553}$$

or nearly 1 part in 43,000 (> 15 bits). As a result, it appears that the requirement to measure radial velocity to an rms error of $0.01/3 = 0.0033$ m/s during docking is both unrealistic and inconsistent with the other accuracy requirements. We will therefore assume that the radial velocity accuracy required during docking is the same as that during rendezvous - $3\delta v_r = 0.1$ m/s.

We will now show that the limit on the tracking rate is set by the accuracy requirement on range rate (radial velocity) rather than on angular rate (angular velocity). From Equations 28, 34, 37, and 38, the ratio of signal-to-noise ratios for angular and range measurements is given by

$$A = (S/N)_\theta^{1/2}/(S/N)_r^{1/2} = 2\sqrt{2}\,\pi\,\left(\frac{\theta}{\lambda}\right)\left(\frac{\delta v_r}{\delta\omega}\right). \qquad (39)$$

IDCA-28

During rendezvous, the minimum value of $\theta = 9 \times 10^{-5}$ (at r = 1000 m) and the maximum value of $\theta = \theta_d = 4.9 \times 10^{-4}$ (at r = 100 m). In addition, $3\delta v_r$ = 0.1 m/s and $3\delta \omega = 1 \times 10^{-4}$ radians/second. For a minimum λ = 20 m (f = 15 MHz, which requires a three-tone system), this gives us

$$A = 0.040 \text{ (min.)}, \quad 0.218 \text{ (max.)}$$

During docking, $\theta = \theta_d = 4.9 \times 10^{-4}$, $3\delta v_r$ = 0.1 m/s, and $3\delta \omega = 1 \times 10^{-4}$ radians/second. For λ = 20 m, we then have

$$A = 0.218.$$

The signal-to-noise ratio needed for tracking is therefore set by the range rate accuracy for both rendezvous and docking.

As a result, the relationship between tracking rate m_r = $1/\Delta t$ and laser power ϕ_t is contained in the equation

$$(S/N)^{1/2} = \frac{\lambda}{2\sqrt{2}\ \delta v_r\ \Delta t}. \tag{40}$$

During rendezvous, the noise bandwidth B in the equation for (S/N) is given by B = 2/Δt (Section 2.4.4). In addition, the returns from three retro-reflectors are detected, but three tone frequencies are used. As a result, the received signal power is given by

$$\phi_r = \frac{0.25\ \phi_t}{(1000)^4} \left(\frac{0.050 \times 0.050}{3 \times 10^{-2} \times 9 \times 10^{-5}}\right)^2 = 2.143 \times 10^{-7}\ \phi_t$$

at the maximum rendezvous range of 1000 m. The signal-to-noise ratio is then given by

$$\frac{S}{N} = \frac{0.016(2.143 \times 10^{-7})^2\ \phi_t^2\ \Delta t}{16 \times 2 \times 1.602 \times 10^{-19}(0.5 \times 3 \times 2.143 \times 10^{-7}\ \phi_t + 1.007 \times 10^{-9})}$$

For λ = 20 m and $3\delta v_r$ = 0.1 m/s, Equation 40 then yields for a rendezvous

$$m_r^3 = \frac{3.145 \times 10^{-2}\ \phi_t^2}{3.215 \times 10^{-7}\ \phi_t + 1.007 \times 10^{-9}}$$

The resultant laser powers required for various rendezvous tracking rates are plotted in Figure 2.6.2-1 and listed in the following tabulation.

Tracking Rate $m_r(s^{-1})$	Laser Power ϕ_t (W)
21.2	1×10^{-1}
18.7	7×10^{-2}
16.6	5×10^{-2}
15.4	4×10^{-2}
13.85	3×10^{-2}
11.9	2×10^{-2}
10.7	1.5×10^{-2}
9.06	1×10^{-2}
8.25	8×10^{-3}
7.28	6×10^{-3}
6.70	5×10^{-3}
6.03	4×10^{-3}
5.24	3×10^{-3}
4.24	2×10^{-3}
3.62	1.5×10^{-3}
2.87	1×10^{-3}

For docking, the maximum range r is reduced to 100 m and the bandwidth is increased to $B = 6/\Delta t$ (Section 2.4.4). In addition, measurements must be made on all three retro-reflectors, and the received signal power is attenuated by $(\theta_d/\theta_r)^2$. Under these conditions, we obtain

$$\phi_r = \frac{0.25 \ \phi_t}{3(100)^4} \ (\frac{0.05 \times 0.05}{3 \times 10^{-2} \times 5.4 \times 10^{-4}})^2 \ (\frac{0.49}{0.54})^2 = 1.634 \times 10^{-5} \ \phi_t \ ,$$
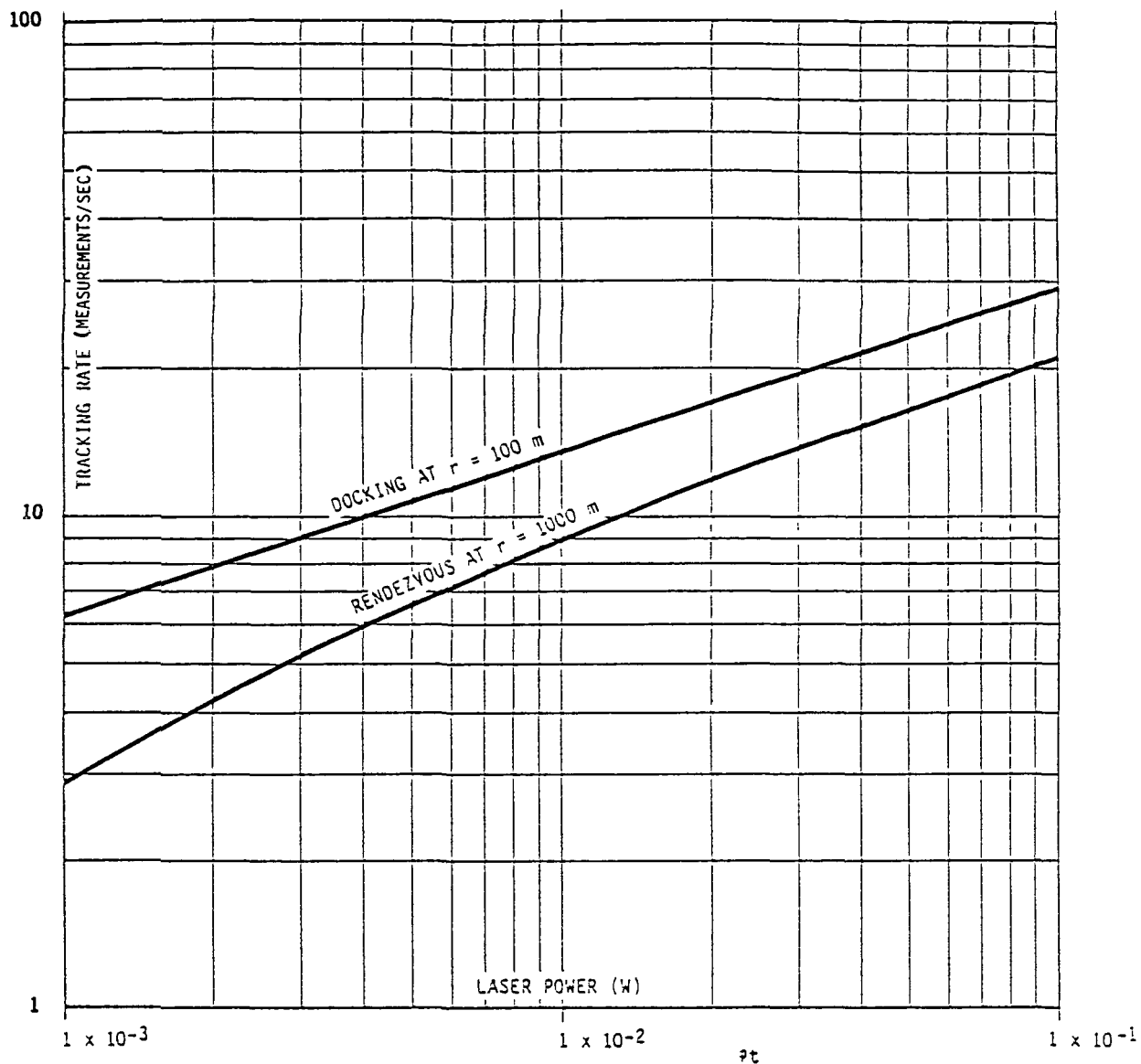
and

$$\frac{S}{N} = \frac{2.778 \times 10^{-5} \ \phi_t^2 \ \Delta t}{2.4511 \times 10^{-5} \ \phi_t + 1.007 \times 10^{-9}}$$

For $\lambda = 20$ m and $3\delta v_r = 0.1$ m/s, Equation 40 then yields for docking

$$m_r^3 = \frac{6.1733 \ \phi_t^2}{2.4511 \times 10^{-5} \ \phi_t + 1.007 \times 10^{-9}}$$

The resultant laser powers required for various docking tracking rates are plotted in Figure 2.6.2-1 and listed in the following tabulation.

IDCA-31

TRACKING RATE (MEASUREMENTS/SEC)

100

10

1

DOCKING AT r = 100 m

RENDEZVOUS AT r = 1000 m

LASER POWER (W)

1×10^{-3} 1×10^{-2} 1×10^{-1}

P_t

$P_b = 1.007 \times 10^{-9}$ W

$D_r = 0.050$ m, $D_f = 0.050$ m

$R = 0.016$ AW^{-1}, $\tau = 0.25$

$\delta V_r = 0.1$ ms^{-1}, $\lambda = 20$ m

$\theta_t = 3 \times 10^{-2}$, $\theta_f = 4 \times 10^{-5}$, $\theta_d = 4.9 \times 10^{-4}$

$B = 2 m_r$ (rendezvous), $6m_r$ (docking)

Figure 2.6.2-1.   Laser Power For Docking Tracking Rates

Rev. A

Tracking Rate $m_r(s^{-1})$	Laser Power ϕ_t (W)
29.3	1×10^{-1}
26.0	7×10^{-2}
23.3	5×10^{-2}
21.6	4×10^{-2}
19.6	3×10^{-2}
17.1	2×10^{-2}
15.6	1.5×10^{-2}
13.6	1×10^{-2}
12.6	8×10^{-3}
11.4	6×10^{-3}
10.8	5×10^{-3}
9.99	4×10^{-3}
9.07	3×10^{-3}
7.90	2×10^{-3}
7.16	1.5×10^{-3}
6.23	1×10^{-3}

Retention of the requirement $\delta v_r = 0.01/3$ m/s during docking would reduce all of the above tracking rates by a factor of $(100)^{1/3} = 4.64$.

2.6.3　Signal-to-Noise Ratios

Both acquisition range (Section 2.6.1) and tracking rate (Section 2.6.2) can be expressed in terms of signal-to-noise ratio (S/N). We will therefore determine the levels of laser power required for various (S/N)'s under three conditions: (a) acquisition at r = 1000 m, (b) rendezvous at r = 1000 m, and (c) docking at r = 100 m. We will assume that the required tracking rate is five sets of measurements (azimuth, elevation and range) on each target every second. (There is one target during acquisition, and there are three targets during docking.)

For the first condition, the equations developed in Section 2.6.1 give us

$$\frac{S}{N_1} = \frac{1.265\ \phi_t^2}{3.215 \times 10^{-7}\ \phi_t + 1.007 \times 10^{-9}}$$

at r = 1000 m. For the second condition, the equations in Section 2.6.2 give us

$$\frac{S}{N_2} = \frac{28.667\ \phi_t^2}{3.215 \times 10^{-7}\ \phi_t + 1.007 \times 10^{-9}}$$

at r = 1000 m. And for the third condition, the equations in Section 2.6.2 yield

$$\frac{S}{N_3} = \frac{5.556 \times 10^4 \ \phi_t^2}{2.451 \times 10^{-5} \ \phi_t + 1.007 \times 10^{-9}}.$$

The levels of laser power required for various values of all three signal-to-noise ratios are shown in Figure 2.6.3-1.

The tracking accuracy that corresponds to a (S/N) level for the second and third conditions is given by Equation 40 in terms of the rms radial velocity uncertainty.

$$\delta v_r = \frac{50}{2 \ (S/N)^{1/2}} m/s$$

for a measurement (lowest) wavelength $\lambda = 20$ m.

2.7 SPECTRAL RESPONSE CURVES

The spectral response curves for the various red sensitive multi-alkali materials are shown in Figure 2.7-1 and for GaAs (III-V compound), in Figure 2.7-2. The MA multi-alkali photocathodes form a continuous series of materials with continuously varying compositions and spectral responses.
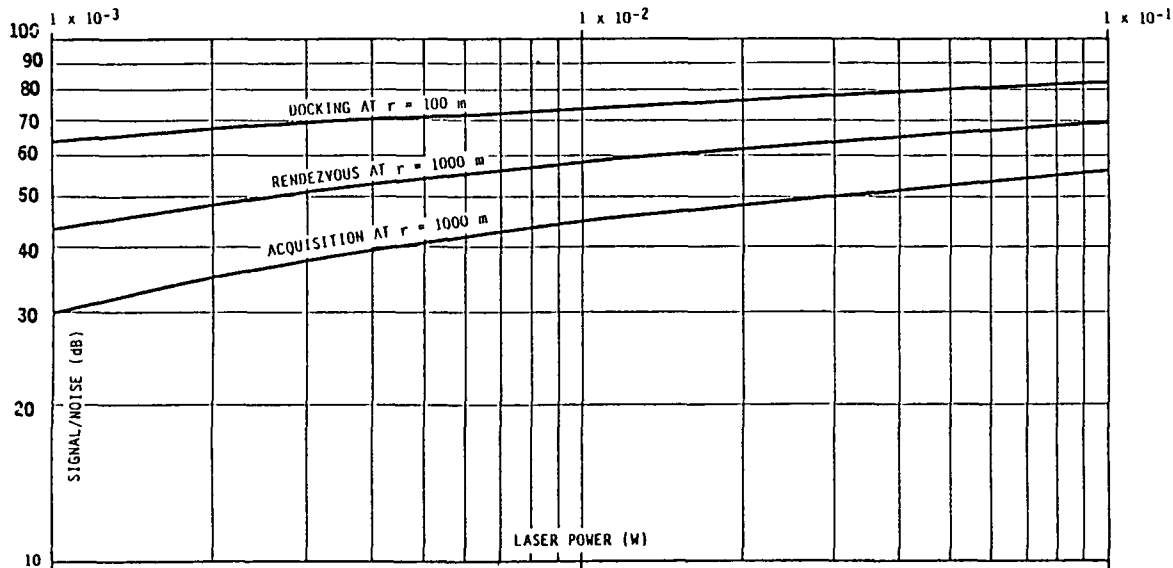
$\phi_b = 1.007 \times 10^{-9}W$, $R = 0.016$ AW^{-1}, $\tau = 0.25$, $B = 2.04 \times 10^3$ Hz (ACQUISITION), 10 Hz (rendezvous), 60 Hz (docking)

$D_r = 0.050$ m, $D_f = 0.050$ m, $\theta_t = 3 \times 10^{-2}$, $\theta_f = 4 \times 10^{-5}$, $\theta_d = 4.9 \times 10^{-4}$

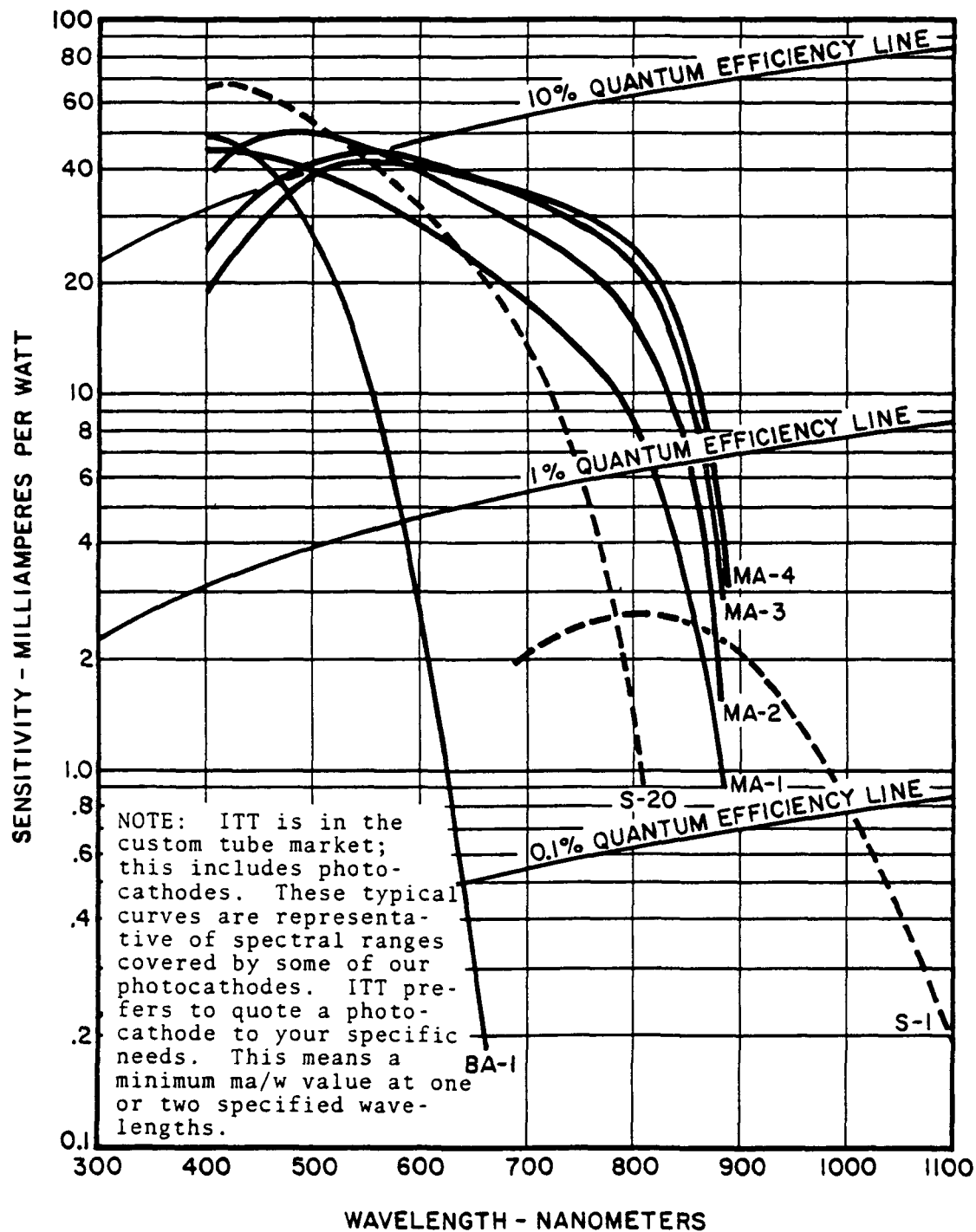Figure 2.6.3-1. Laser Power Versus S/N Ratio

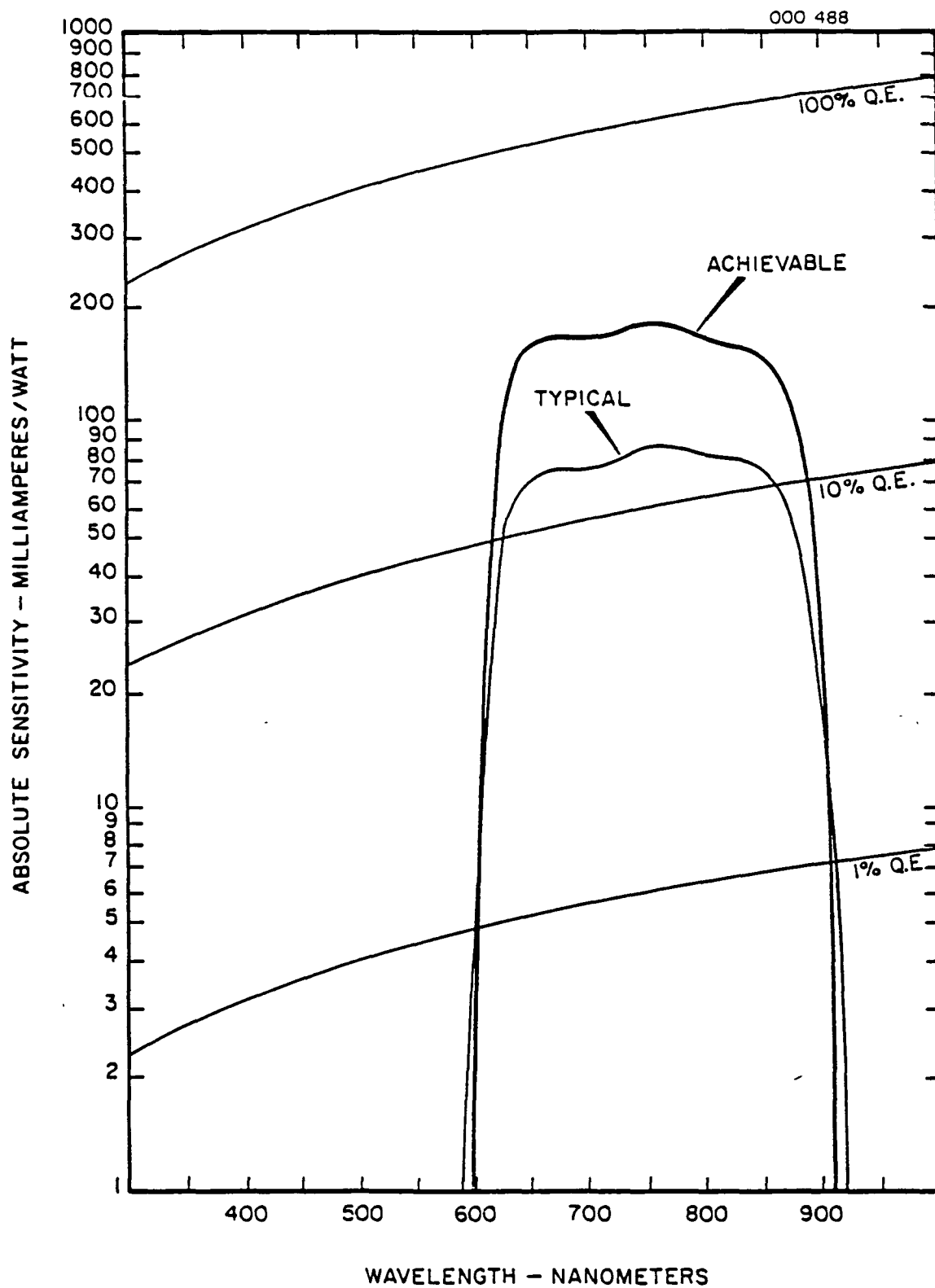**Figure 2.7-1. Typical Spectral Response Characteristics**

Figure 2.7-2. III-V Photocathode Spectral Response

Section 3

SCAN SYSTEM

The design of a rendezvous and docking sensor system must meet the combined requirements of two operating modes. These are (1) search, acquisition, and tracking for rendezvous and (2) tracking for docking. Rendezvous will occur at ranges greater than 100 meters. The maximum range considered here will be 1000 meters. Parameters being measured during rendezvous are range, range-rate, angle, and angle-rate of the satellite with respect to the receiver reference. During docking, the range, range-rate, angle, and angle-rate to each reflector on the satellite must be measured. Docking range will be from 3 to 100 meters.

3.1 SYSTEM DESCRIPTION

The general configuration of the systems that will be considered is shown in Figure 3.1-1a or 3.1-1b. The transmitter and receiver are separately deflected in both configurations. In Figure 3.1-1a, the transmitter beam is deflected before it is combined with the receiver beam. This is the configuration used by a piezoelectric deflection system with deflection magnification. It could also be used by other deflection systems. In Figure 3.1-1b, the transmitter beam is deflected after it is combined with the receiver beam. This approach will usually have less obscuration of the receiver beam; this will be discussed later. The deflection systems considered here will be the piezoelectric system as shown in Figure 3.1.1a and a two-axis gimbaled system located as shown in Figure 3.1.1b.

The receiver will consist of an image dissector tube (IDT) detector and associated optics and electronics. The field-of-view (FOV) of the receiver will be 20° x 20°, which is the FOV of the system. The 25 mm IDT can provide this FOV if a 28 mm FL lens is used; see Section 2.6. If a 57 mm IDT, e.g., F4100, is used, a 70 mm FL lens can be used. The instantaneous field-of-view (IFOV) of the receiver is set by the size of the aperture in the IDT. The receiving IFOV used will be 0.002 radians. Therefore, the aperture in the 25 mm (F4012) IDT will be 0.0023 inch and, for the 57 mm IDT, the aperture will be 0.0057 inch.

3.2 SEARCH AND ACQUISITION

The location of the target satellite will be known to within $\pm$ 10° in both the X and Y coordinates of the rendezvous and docking system. The 20° square field will be scanned by a back-and-forth raster scan with the transmitter and receiver scans tracking each other. The accuracy of the tracking between the beams will depend on the divergence of the transmitter beam. If the beam divergence is 2 mrad, the tracking accuracy between the beams will have to be $\pm$ 0.1 mrad or less to avoid missing a target when using 10 percent line-to-
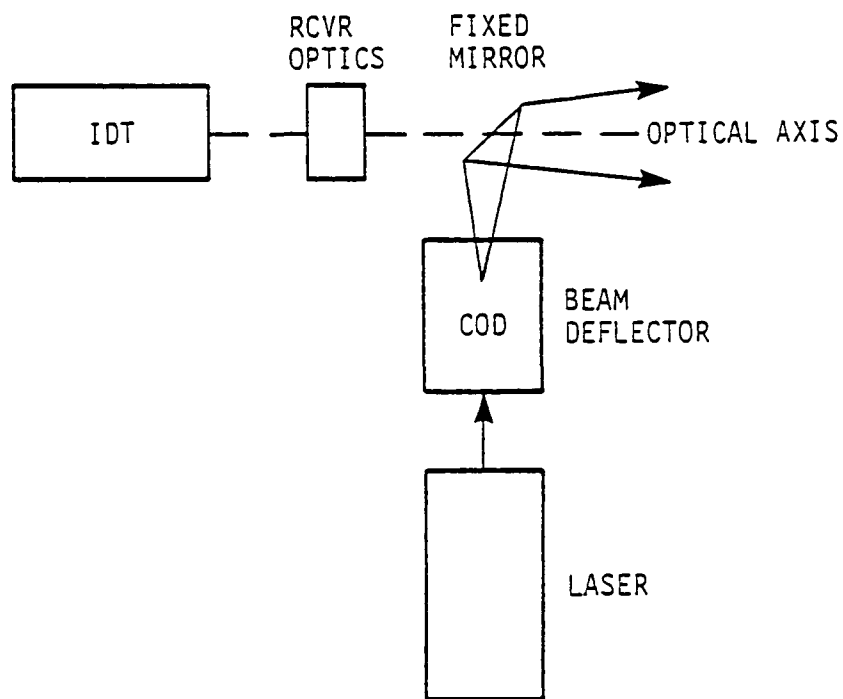
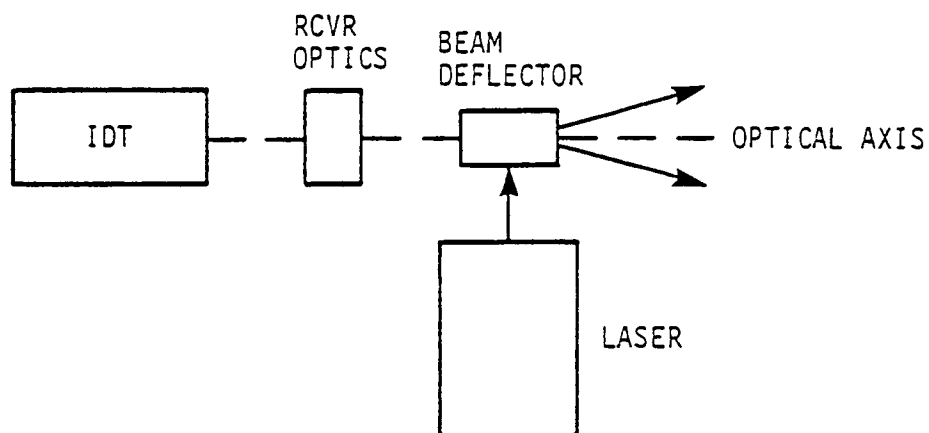Figure 3.1-1a. Off-Axis Transmitter Beam Deflection

Figure 3.1-1b. On-Axis Transmitter Beam Deflection

Rev. A

line overlap. If, however, the beam divergence is 30 mrad, the tracking accuracy then must be $\pm$ 14 mrad or less.

Covering 20° (349 mrad) with a 2 mrad beam and 10 percent overlap will require 183 scan lines. To maintain acceleration requirements during scanning similar to those required for docking, it is recommended that a frame time for one raster be five seconds. This makes the line time 27 ms. The line time will be divided into 20 ms for scan and 7 ms for turnaround. If faster acquisition is required, the IFOV can be increased with some loss in signal to noise. A 20° circular FOV can be scanned in three seconds by using a spiral scan with a constant tangential scanning velocity of 1°/ms, which is the same scanning velocity as the raster scan.

3.3   DOCKING

The docking phase will begin at about 100 m. During docking, each of the three reflectors will be tracked in range and azimuth so that the target satellite's position and orientation can be determined. Tracking will continue to a minimum range of about three m.

At the ranges for docking operation, one must consider the differences in operation in the far field and the near field. The transition from far field to near field occurs when the diameter of the laser beam at the reflector is equal to the diameter of the reflector. In the far field, i.e., the beam is larger than the reflector, either transmitter deflection or receiver deflection can be used because different parts of the reflector correspond to different ray angles in the transmitter beam, and therefore, different positions in the receiver image plane.

This is not the case in the near field. All the receiver can measure is the center of the transmitter beam, which is already known. This is illustrated for a narrow beam into a corner cube in Figure 3.3-1. If the corner cube is in position A, the return beam will be R_A. If the corner cube is in position B, the return beam will be R_B. But R_A and R_B are parallel beams and, therefore, will be imaged at the same spot in the receiver image plane. This means that moving the corner cube from position A to position B will cause no image motion in the receiver. The same argument holds true for a multi-element retro-reflector. This means that receiver deflection cannot be used to track the reflectors when operating in the near field.

There are two ways to circumvent this problem. The first is to use transmitter beam deflection to track the reflectors in the near field (and perhaps in the far field also). This technique will be slower than receiver tracking because the transmitter deflection is not as agile as the receiver deflection.

The second way to circumvent the problem is to increase the divergence of the transmitter beam so that the system is always
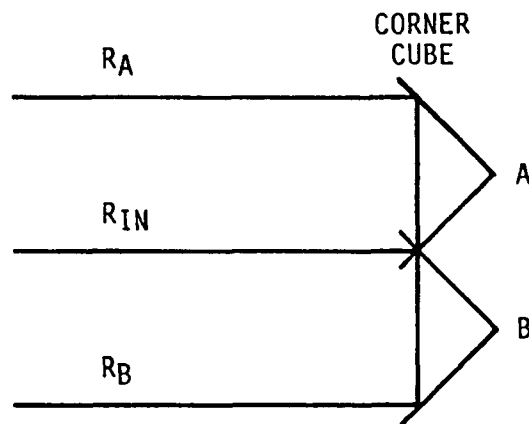
Figure 3.3-1. Corner Cube Motion Versus Return Beam Angle
in the Near Field

operating in the far field. At 3 m, the angular size of a 50 mm
reflector is 17 mrad. The beam must be somewhat larger. A value of 30
mrad has been selected. This beam divergence will ensure that the
system always operates in the far field, reducing the tracking accuracy
required between the transmitter and receiver and still yielding a
signal-to-noise ratio of 29 dB at 1 Km from a single corner cube when
using a 28 mm receiver lens, a 50 mm corner cube, an MA-4 photocathode,
and 40 mW of laser power. Using a multi-faceted reflector with .001
rad diffraction limit, the S/N is reduced to -4 dB. Therefore, it is
recommended that quality corner cubes be used for the reflectors and
that the divergence of the transmitter be about 30 mr.

3.4   TRANSMITTER DEFLECTION SELECTION

        The deflection of the transmitter beam can be accomplished
by the configuration shown in Figure 3.1-1a or the one in Figure
3.1-1b. The off-axis deflection configuration, Figure 3.1-1a, can be
implemented by a two-axis, gimbaled deflection system or a
piezoelectric bimorph deflection system with optical scan magnification
as described in the RCA study (Reference 2). One significant problem
with the off-axis system is the relatively large obscuration of the on-
axis mirror. This is shown in Figure 3.4-1. The on-axis obscuration
equals r + r′ and is given by

Figure 3.4-1. Obscuration for Off-Axis Deflection

Figure 3.4-2. High-Speed, Two-Axis Scanner

$$r + r' = \frac{2R \tan \theta}{1 - (\tan \theta)^2}$$

where R is the distance from the apparent center of deflection (COD) of the deflection system to the optical axis of the receiver and 2θ equals the total deflection angle of the output beam. The size of the mirror must be greater than 28 mm on a side for R = 3 inches and θ = 10°. This will totally obscure the receiver optics for a 25 mm IDT receiver. See Section 3.1. This will obscure a significant amount of energy from far field target when using a larger IDT and larger optics. When the target is in close, the obscuration will distort the images of the corner cubes on the IDT and cause errors in the location of the center of each corner cube. Also, at close range, a significant amount of the total laser power will be intercepted by the mirror and fed back into the laser cavity. This can cause spurious operation of the laser. For these reasons, it is recommended that the off-axis deflection system not be used.

The recommended deflection is the on-axis configuration, using a two-axis, gimbaled scanner. This deflection system is shown in Figure 3.4-2. The view shown is looking directly into the receiver, and the mirror is centered on the optical axis. The aluminum ring supported by the #1 drive motor and position sensor is rotated $\pm$ 5° (mechanical) by the #1 drive motor. The mirror is mounted on a shaft which is rotated $\pm$ 10° (mechanical) by the #2 drive motor. The #2 drive motor and position sensor are mounted to the aluminum ring. The two-position sensors measure the angular position of their respective shafts and send this information back to their respective drive amplifiers to close the loop.

The mirror will be tilted toward the right and the laser will be located to the right and in front of the scanner assembly. This configuration will deflect the beam 2° for each 1° of mechanical rotation about the #1 drive axis. The deflection about the #2 drive axis is one for one. This configuration was selected because the inertia about the #1 drive axis is about 250 times greater than the inertia about the #2 drive axis.

The optimum step-and-settle routine is defined here as that routine which requires the minimum peak torque from the drive motor when moving from position A to position B in time T. Ideally, this routine consists of a constant positive torque for the first half of the period (T/2) and an equal negative torque for the second half of the period in which the amplitude of the torque is proportional to the distance between A and B. Ideally, the velocity will be zero precisely when the scanner reaches B. This is an open-loop routine and probably will not work adequately because of friction and system errors. However, this routine can be implemented by using a closed-loop; this forces the scanner to follow the routine.

The equations of motion for this routine are as follows:

IDCA-36

$$\theta = \Delta\theta \, (4X^2 - 1) \qquad\qquad 0 \le X < \tfrac{1}{2}$$

$$-\Delta\theta \, (4X^2 - 8X + 3) \qquad \tfrac{1}{2} \le X \le 1$$

$$\dot{\theta} = \frac{8\Delta\theta}{T} X \qquad\qquad 0 \le X < \tfrac{1}{2}$$

$$= \frac{8\Delta\theta}{T} (1 - X) \qquad\qquad \tfrac{1}{2} \le X \le 1$$

$$\ddot{\theta} = \frac{8\Delta\theta}{T^2} \qquad\qquad 0 \le X < \tfrac{1}{2}$$

$$= -\frac{8\Delta\theta}{T^2} \qquad\qquad \tfrac{1}{2} \le X \le 1$$

where $X = t/T$

$2\Delta\theta$ = angular distance between A and B and θ, $\dot{\theta}$ and $\ddot{\theta}$ are angular position, angular rate, and angular acceleration, respectively. The step-and-settle routine will be implemented by the same positive and negative torque signal described above. The actual angular position will be monitored and compared to the ideal angular position. The difference is an error signal and will be used to modulate the torque forcing the scanner to follow the routine so that the scanner arrives at position B at time T with zero velocity.

This control function can be accomplished by either analog or digital processing. However, it is assumed that system operation will be controlled by a microprocessor, which will be used to control the step-and-settle sequence.

A preliminary design has been made of the scanner shown in Figure 3.4-2. For the design, it was assumed that the receiver optical diameter is 75 mm. The inertia of the scanner about the #1 drive axis is .033 oz-in-sec^2. The inertia about the #2 drive axis is 1.32×10^{-4} oz-in-sec^2. The maximum angular acceleration for the #1 drive is 775 rad/sec^2 for an angular step of 10° and a step-and-settle time of 0.03 second. The maximum angular acceleration for the #2 drive is 1550 rad/sec^2 for an angular step of 20°. Therefore, the maximum torque required will be 26 oz-in for #1 drive motor and .2 oz-in for the #2 drive motor. The motor selected for the #1 drive motor has a peak torque rating of 40 oz-in and the motor selected for the #2 drive motor has a peak torque rating of 1.3 oz-in. Therefore, the system can readily step and settle in 30 msec by using the controlled step-and-settle sequence.

The tracking sequence will consist of three parts. The first part will be the step-and-settle from target A to target B. The scan will stop at the last known Y position of target B and 15 mrad to the left of the X position. The second part will be a 30 mrad scan along the X axis through the target. The scan will then center on the

X location of the target and scan $\pm$ 15 mrad through the target along the Y axis. The third part is to go to the center of the target and measure the range. The time required for each of these parts is as follows:

Step and Settle		.03 s
X Scan	.015 s	
Y Scan	.015 s	
		.03 s
Ranging		.007 s
	Total	.067 s

Therefore, the system can measure the angular position and range of 15 targets per second.

Section 4

CAMERA FREQUENCY RESPONSE

The video frequency response of the image dissector camera constructed for this study program is documented in the oscilloscope photographs included in this section.

4.1 TEST DATA

The signal source for these measurements was a gallium aluminum arsenide IR emitter (RCA type C86043E) connected as shown in Figure 4.1-1. The spectral output of this device is peaked at 820 nanometers and was intensity modulated by a RF sweep generator. The photographs show the detected video signal out of the camera video amplifier. Markers are at 2, 5, 10, 15, and 20 MHz.

Data were taken at the following image dissector electron multiplier gains. See the listed figure for an oscilloscope picture of each.

	GAIN	MULTIPLIER VOLTAGE
Figure 4.1-2	1×10^5	950 Vdc
Figure 4.1-3	2×10^5	1030 Vdc
Figure 4.1-4	5×10^5	1150 Vdc
Figure 4.1-5	1×10^6	1250 Vdc
Figure 4.1-6	2×10^6	1350 Vdc

It was noted that, at high levels of multiplier gain, combined with high levels of input signal, the frequency response peak shifted to the left, while the high frequencies fell off. This apparently is caused by high signal currents in the tube anode and last dynode, i.e., current starvation in the bleeder. Reducing the input signal level at high multiplier gain restores the video bandwidth. See Figure 4.1-7.
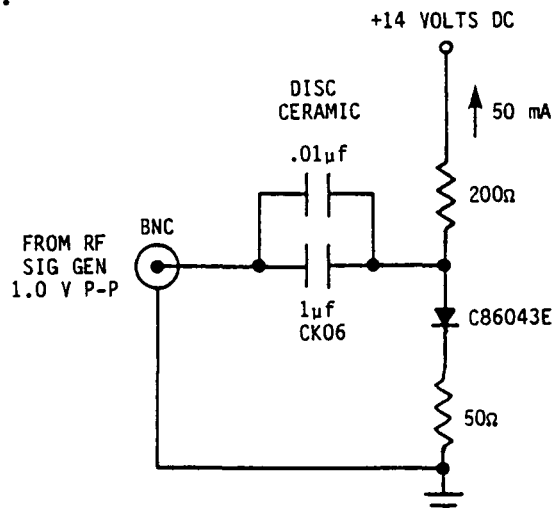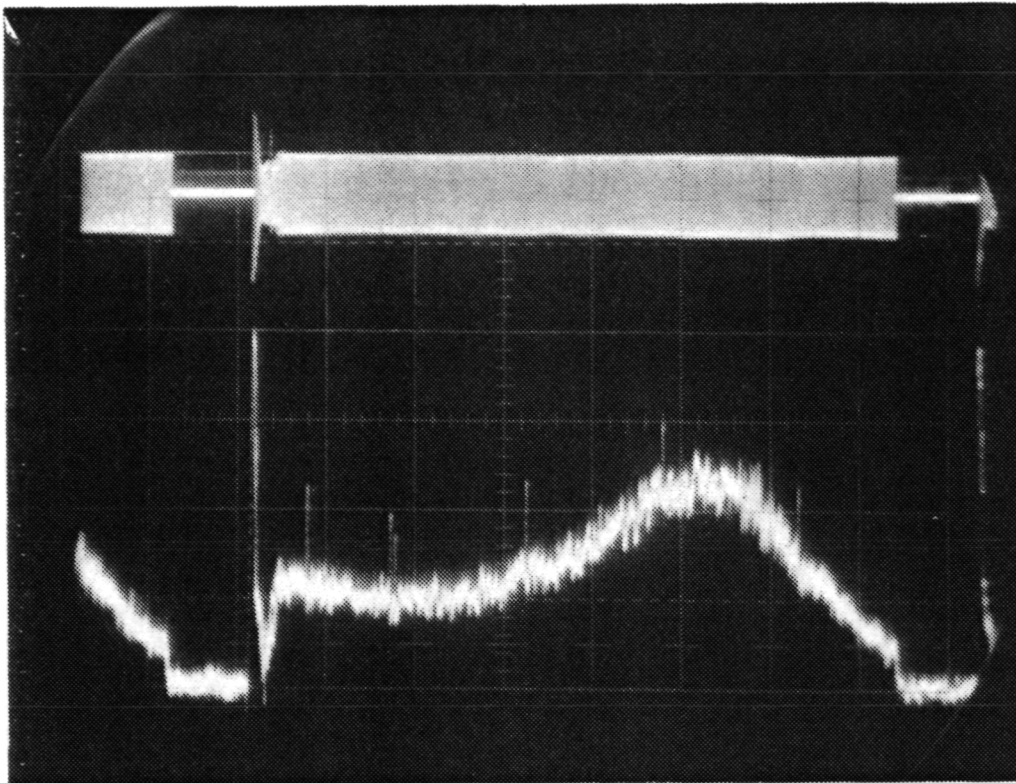
Figure 4.1-1. Test Source Schematic

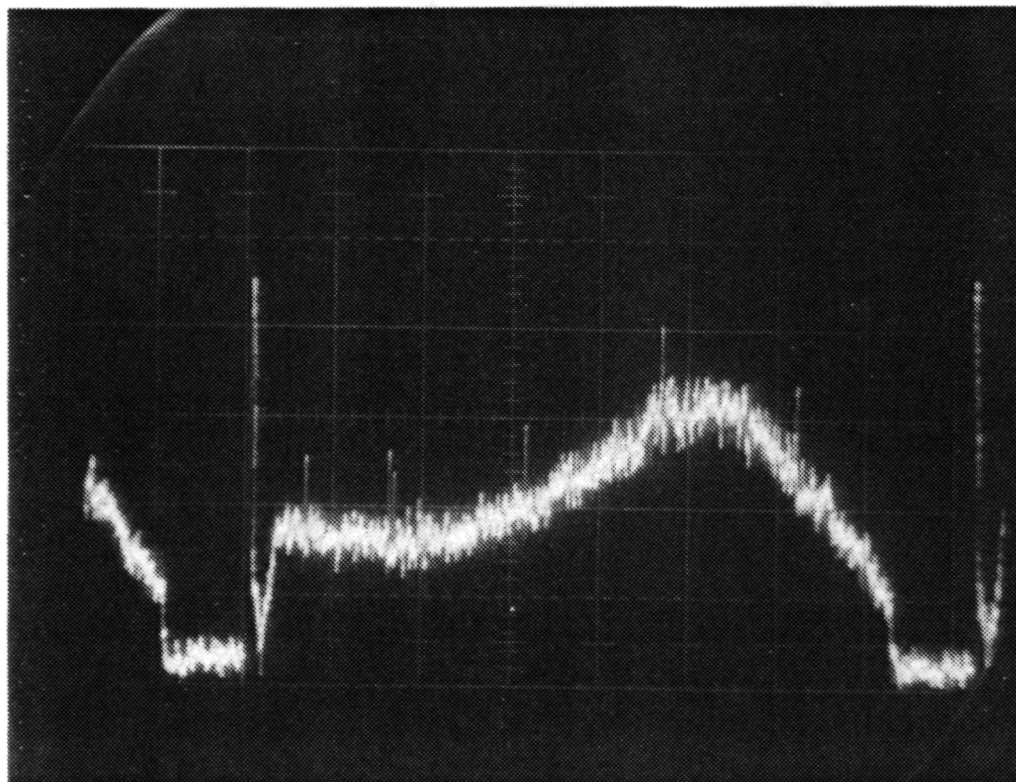Figure 4.1-2. Video Response at Gain 1×10^5
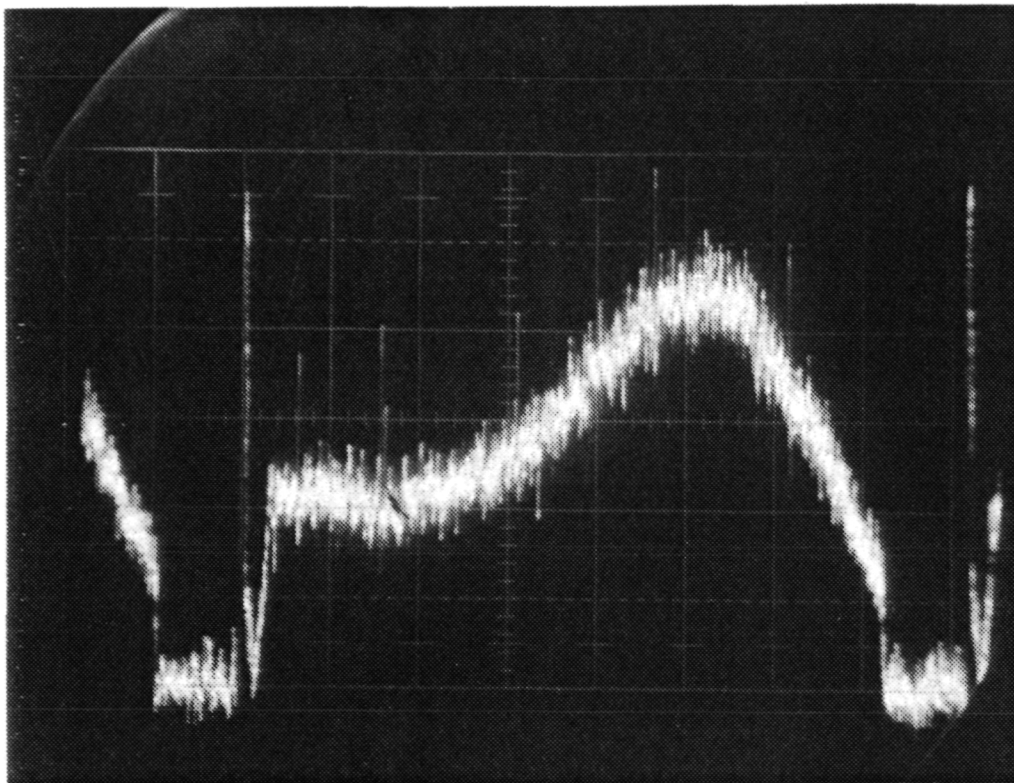

Figure 4.1-3. Video Response at Gain 2×10^5

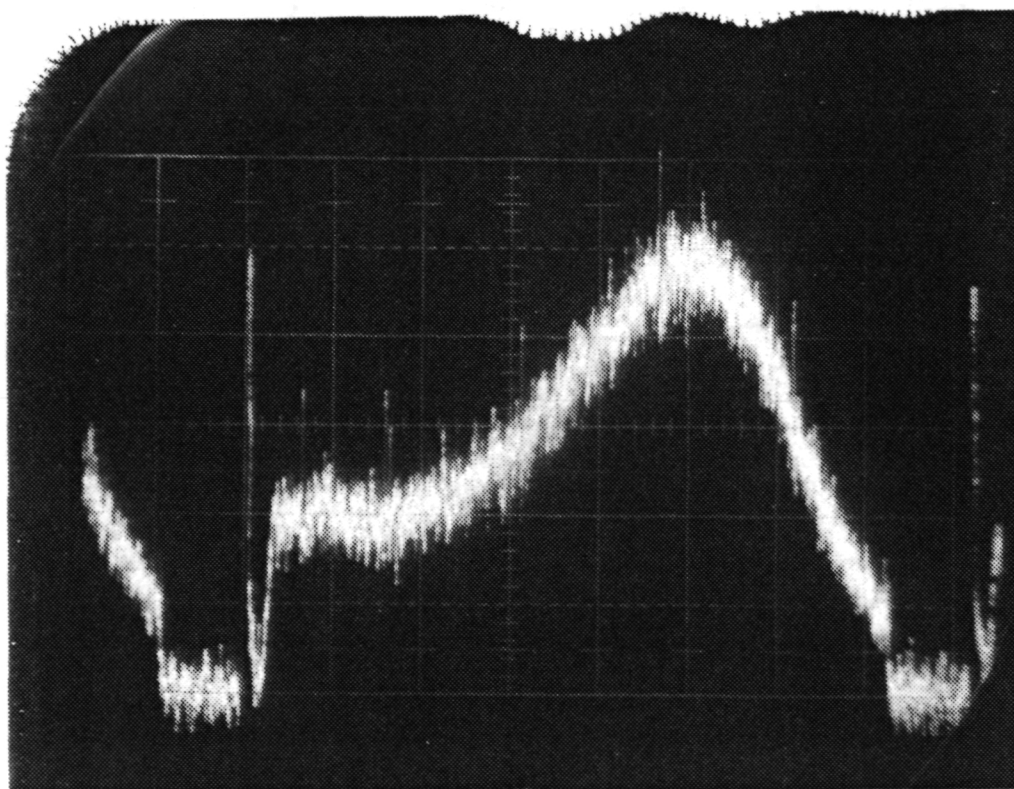Figure 4.1-4. Video Response at Gain 5×10^5

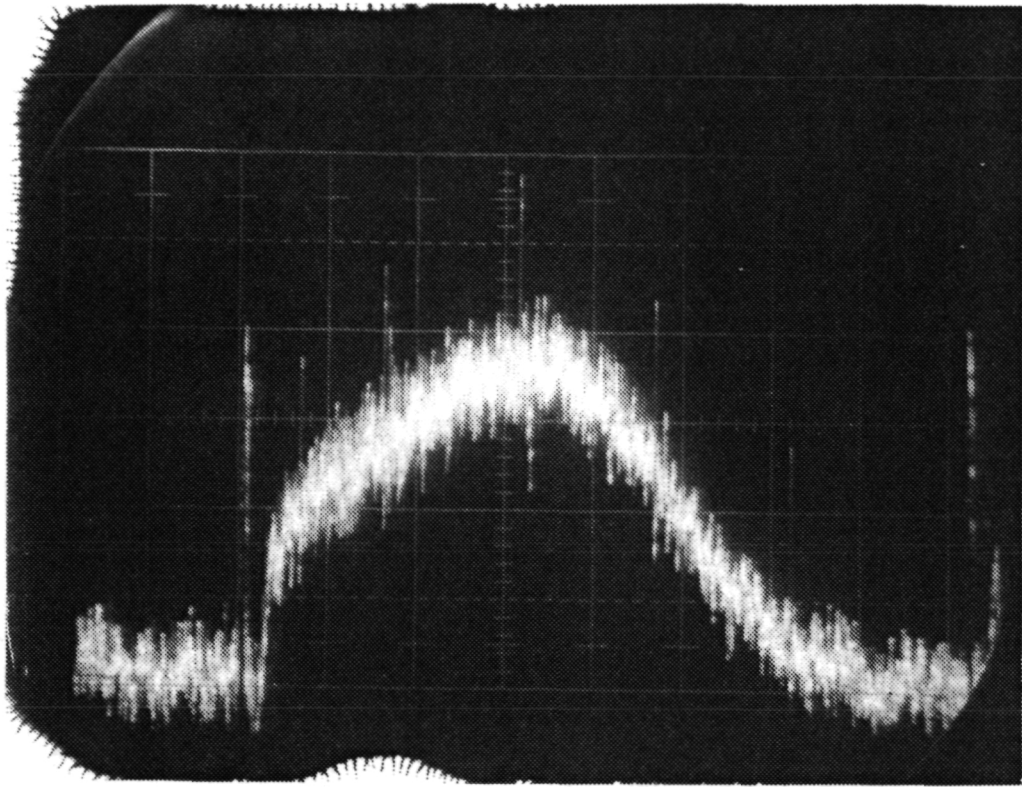Figure 4.1-5. Video Response at Gain 1×10^6

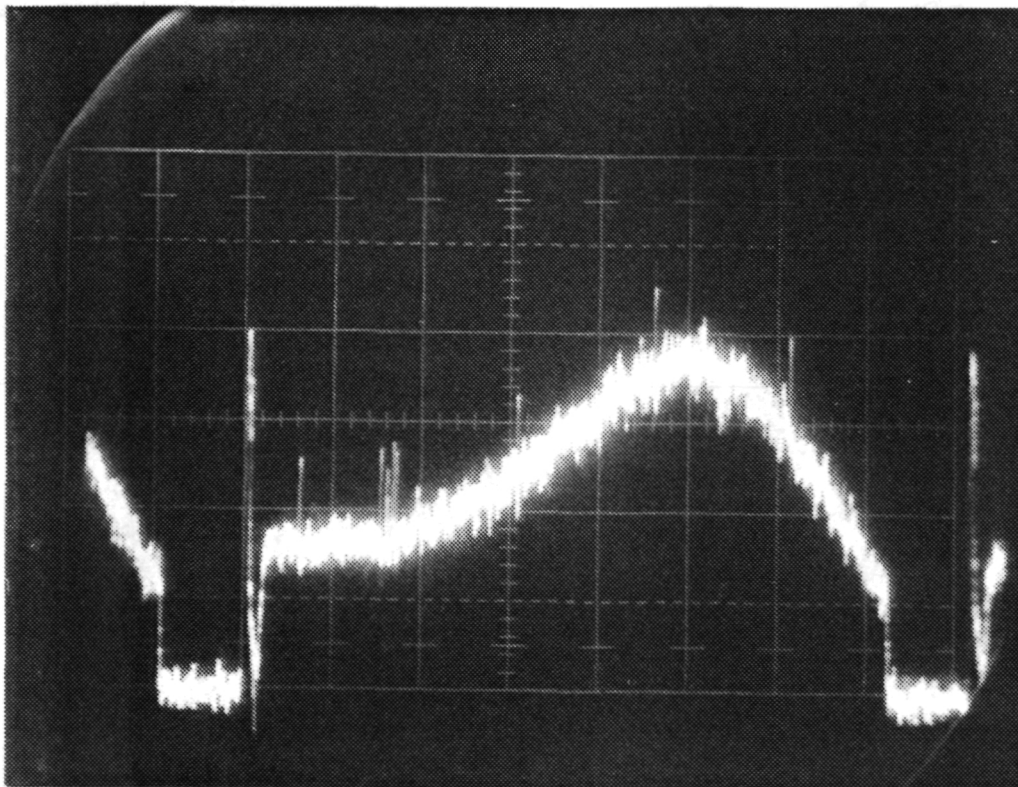Figure 4.1-6. Video Response at Gain 2 x 10^6 (Output Overloaded)

Figure 4.1-7. Video Response at Gain 2 x 10^6 (Reduced Input Signal)

REFERENCES

1. H. D. Eckhard, Simple Model of Corner Reflector Phenomena, Appl. Opt. <u>10</u>. 559 (1971).

2. R. J. Laurie and F. Sterzer, Advanced Multipurpose Rendezvous Tracking System Study, June 1, 1982, RCA Laboratories (Princeton, NJ, 08540) for NASA/JSC under Contract NAS9-16252, Section 5.5 and 6.2.

3. Ref. 2, Table 2-4, p. 11.

4. D. Botez, D. J. Channin, and M. Ettenberg, High-Power Single-Mode A GaAs laser diodes Opt. Engr. <u>21</u>, 1066 (1982).

5. R. J. Laurie and F. Sterzer, Advanced Multipurpose Rendezvous Tracking System Study, June 1, 1982, RCA Laboratories (Princeton, NJ 08540) for NASA/JSC under Contract NAS9-16252, Section 6.4.

6. W. G. Knorr, NASA/JSC Rendezvous and Docking Experiment, August 30, 1983.

7. C. W. Allen, Astrophysical Quantities, Second Edition, University of London, The Athlone Press, 1963, p. 145.

8. H. Neckel and D. Labs, Improved Data of Solar Irradiance from 0.33 to 1.25 μm, Sol. Phys. <u>74</u>, 231 (1982).

9. Ref. 5, Figure 4-8 (p. 32).

10. Proc. SPIE <u>268</u>, Imaging Spectroscopy (1981).

11. Opt. Engr. <u>20</u>, November/December 1981.